

# University of Cincinnati

Date: 5/13/2011

I, Sowmya Sukhavasi, hereby submit this original work as part of the requirements for the degree of Master of Science in Computer Engineering.

It is entitled:

**"Zinc Chip" Reader for Point-Of-Care Quantification of Zinc in Blood Serum**

Student's name: **Sowmya Sukhavasi**

This work and its defense approved by:

Committee chair: Fred Beyette, PhD

Committee member: Ian Papautsky, PhD

Committee member: Carla Purdy, C, PhD



1730

# Zinc Chip Reader for Point-Of-Care Quantification of Zinc in Blood Serum

A thesis submitted to the  
Graduate School  
of the University of Cincinnati  
in partial fulfillment of the  
requirements for the degree of

## **Master of Science**

in the Department of Electrical and Computer Engineering  
of the College of Engineering and Applied Science

By

**Sowmya Sukhavasi**

B.Tech(ECE), JNTU, India, 2008.

May 2011

**Thesis Advisor and Committee Chair: Dr. Fred R. Beyette Jr.**

## Abstract

Zinc is a very important trace element required for normal functioning of hormones, transcription-related factors and multiple enzymes<sup>1</sup>. Studies have demonstrated abnormally low Zinc levels as a predominant characteristic of pediatric septic shock and supplementation of Zinc has been proposed as a therapeutic strategy to treat critically ill patients<sup>2</sup>. Use of Zinc supplementation as a therapeutic strategy would require frequent measurement of Zinc in blood serum. Currently Atomic Absorption Spectroscopy (AAS) or Inductively Coupled Plasma Mass Spectroscopy (ICP-MS) are the only accepted methods used for monitoring Zinc levels. These techniques are accurate but often require sending samples to a centralized external laboratory which increases the turn-around time from hours to days; This inadequate monitoring time frame could lead to over-supplementation resulting in critical situations involving heavy metal (Zinc) toxicity. Thus, sending blood samples to an external laboratory and waiting on the results is not an efficient or clinically acceptable process. To overcome these difficulties a rapid and reliable Point-Of-Care system has been developed for quantification of Zinc in blood serum samples. It consists of a Lab-On-Chip sensor and a Zinc chip reader. The electroanalytical technique used for Zinc quantification is square wave anodic stripping voltammetry.

The primary focus of this work was to develop a portable and inexpensive Zinc chip reader that can quantify Zn at the patient bedside. Zinc measurement with the system described here has a turn-around time of about 30 minutes. The device is compact (consistent in size with other point-of-care devices and weighs about 0.5lbs. The Zinc chip reader integrates with the sensor. In addition to providing all electronics signals to drive the sensor, the reader detects the current signal associated with the presence of Zinc in the sample and stores the data for

subsequent analysis. The device hardware has been developed using commercially available embedded system components.

This thesis reports on the design and function demonstration of the Zinc chip reader.



## **Acknowledgements**

First and foremost I would like to express my gratitude to my advisor Dr. Fred Beyette for his expert guidance and encouragement towards completing this challenging work. Thank you Dr. Beyette for your advices and support throughout my graduate studies which inspired me to never stop learning.

I would like to thank Dr. Ian Papautsky for his suggestions during the research and for serving on my committee. I would like to thank Dr. Carla Purdy for taking her time out to serve on my committee.

A special thanks to Dr. Ridgway and Preetha for their time and patience during debugging and testing the Instrumentation. I am thankful to all my friends in POCSDL, specially Deepika and Vignesh for patiently listening to me and helping me troubleshoot.

I thank Sahiti, Pratyusha, Priyanka and Bhargava for making Cincinnati a home away from home. I cannot thank enough my best friend Shruthi for being there for me all my life.

I dedicate this work to my loving Husband, Parents and Grand-parents who instilled in me the values of hard work, dedication and inspired me to live life to its fullest. I would like to specially thank my Husband Vamsi, for being there with me through the thick and thin of life, you are my role model and inspiration for life.

# Table of Contents

List of Figures .....	viii
List of Tables: .....	x
INTRODUCTION .....	1
1.1 Overview of pediatric septic shock .....	1
1.2 Point- Of- Care device approach.....	1
1.3 Research objectives.....	2
1.4 Thesis outline .....	3
CHAPTER 2 .....	4
PRINCIPLES AND DESIGN OF INSTRUMENTATION.....	4
2.1 Overview of the three-electrode sensor .....	4
2.2 Electrochemical detection of Zinc .....	5
2.3 Zinc chip reader system design.....	10
CHAPTER 3 .....	13
DEVELOPMENT OF INSTRUMENTATION .....	13
3.1 Flow chart for conducting SWASV .....	13
3.2 The PICDEM™ PIC 18 explorer demonstration board .....	17
3.3 Programming the microcontroller .....	20
3.4 The PIC18F8722 microcontroller .....	21
3.5 The Digital to Analog converter module .....	34
3.6 Construction of the potentiostat .....	36
3.7 Memory module.....	46
3.8 Power supply and Printed Circuit Board.....	50
CHAPTER 4 .....	51
EXPERIMENTAL VERIFICATION .....	52

4.1 Testing using sensor equivalent circuit.....	52
4.2 Experimental set-up .....	52
4.3 Results and discussion .....	54
CHAPTER 5 .....	57
CONCLUSIONS AND FUTURE WORK .....	58
5.1 Conclusion .....	58
5.2 Future work.....	59
References:.....	60



## List of Figures

Figure 1 Functional diagram of the Point-Of-Care system.....	3
Figure 2 (A) Photograph of the electrochemical sensor with connectors and (B) close-up image of the sensor electrodes where AE is Gold auxiliary electrode; RE is Ag/AgCl reference electrode; WE is Bi working electrode .....	4
Figure 3 Stripping potentials of different heavy metals in the working potential window of the sensor .....	6
Figure 4 Square wave anodic stripping voltammetry of Zn on Bi working electrode illustrating the two steps (a) Preconcentration and (b) stripping .....	7
Figure 5 Square wave superimposed on a staircase waveform.....	8
Figure 6 Excitation signal for square wave stripping voltammetry and the current response signal .....	8
Figure 7 Block diagram of the Zinc chip reader .....	10
Figure 8 Flow chart for conducting SWASV .....	15
Figure 9 Flow chart showing the steps involved in each cycle of the stripping phase .....	16
Figure 10 Picture of PICDEM <sup>TM</sup> PIC 18 explorer demonstration board <sup>14</sup> .....	17
Figure 11 List of components of the PICDEM <sup>TM</sup> PIC 18 explorer demonstration board <sup>14</sup> .....	18
Figure 12 Pin diagram of PIC18F8722 and the color coding indicates the connections to various peripheral devices <sup>15</sup> .....	23
Figure 13 PIC18F8722 clock sources and oscillator switching <sup>15</sup> .....	26
Figure 14 Block diagram of PIC18F8722 ADC module <sup>15</sup> .....	28
Figure 15 Configuration of ADCON0 and ADCON1 registers of the ADC module <sup>15</sup> .....	29
Figure 16 Configuration of ADCON2 register of the ADC module <sup>15</sup> .....	30

Figure 17 Master - Slave connection in SPI mode <sup>15</sup> .....	33
Figure 18 (A) Circuit diagram of 14-bit DAC (AD7840), (B) Parallel mode timing diagram <sup>16</sup> ..	35
Figure 19 An operational amplifier.....	37
Figure 20 Different feedback configurations of operational amplifiers .....	39
Figure 21 Equivalent circuit of the electrochemical sensor.....	40
Figure 22 Circuit diagram of potentiostat.....	42
Figure 23 +2.5V Level shifter.....	44
Figure 24 Circuit diagram of OP484 .....	45
Figure 25 Circuit diagram of ADG408 multiplexer .....	47
Figure 26 Connections for 25LC256 EEPROM and the microcontroller.....	48
Figure 27 Connections between SD card and the microcontroller .....	49
Figure 28 negative (-5V) power supply circuit diagram.....	50
Figure 29 PCB layout of Zinc chip reader .....	51
Figure 30 V-I characteristics of the device using the sensor equivalent circuit .....	52
Figure 31 Experimental set-up of the Point-Of-Care device .....	53
Figure 32 Voltammogram for 10 $\mu$ M Zn in acetate buffer of pH 6 using Zinc chip reader and wavenow potentiostat.....	54
Figure 33 Voltammogram for SWASV of Zn concentrations from 10 $\mu$ M to 40 $\mu$ M spiked in an acetate buffer of pH6 .....	55
Figure 34 Calibration curve's for the Point-Of-Care device and Wavenow .....	57
Figure 35 Voltammogram for acetate buffer of pH 6 spiked with 15 $\mu$ M Zn and 5 $\mu$ M Cd .....	57
Figure 36 Calibration curve of the Point-Of-Care device.....	58

## List of Tables:

Table 1 Different configurations of PICDEM™ PIC 18 explorer demonstration board <sup>14</sup> .....	20
Table 2 Pin description of PIC18F8722 (only those that are used) .....	24
Table 3 PIC18F8722 oscillator modes <sup>15</sup> .....	27
Table 4 Feedback resistor values and the corresponding current range .....	46
Table 5 Instruction set of 25LC256 EEPROM .....	48
Table 6 Peak current values for different concentrations of Zn.....	56
Table 7 Peak current values for the three Zn concentrations of Point-Of-Care device and wavenow .....	56

# CHAPTER 1

## INTRODUCTION

### 1.1 Overview of pediatric septic shock

In the United States pediatric septic shock is one of the major health problems with 42,367 cases reported per year and mortality rate of 10.3%<sup>3</sup>. Studies have demonstrated abnormally low Zinc (Zn) levels as a predominant characteristic of pediatric septic shock and many other biological processes related to critical illness<sup>4</sup>. Supplementation of Zinc has been proposed as a therapeutic strategy to treat these critically ill patients<sup>2</sup>.

Zinc is a very essential element that affects the functioning of immune system<sup>5</sup>, insulin secretion/action, various hormones and enzymes. Altering Zn homeostasis has been validated in animal models<sup>6</sup>. Studies have indicated that children with pediatric septic shock have demonstrated persistently early abnormal low concentrations of Zn in blood serum. Also, decrease in Zn concentration has been associated with infections and inflammations. Thus, it has been proposed that Zn supplementation is a safe and very effective therapeutic strategy. However, to be an effective therapeutic regimen, Zn supplementation will require an accurate and fast method for the measurement of serum Zn concentration.

### 1.2 Point- Of- Care device approach

Currently Atomic Absorption Spectroscopy (AAS) or Inductively Coupled Plasma Mass Spectroscopy (ICP-MS) are the methodologies used to quantify Zn concentration in blood serum. These quantification methods often require sending blood samples to an external laboratory, involving turn-around times from hours to days. This time consuming methodology for

quantifying Zn is a challenging component to the supplementation strategy. The issue of timely return is particularly important when dealing with critically ill patients as over supplementation might result in critical situations such as heavy metal (Zn) toxicity. To overcome this challenge a portable, rapid and inexpensive Point-Of-Care device that can quantify Zn at patient's bedside is needed. To meet the expectations associated with the clinical need, the point-of-care device must be a relatively small in size/weight and provide a reasonable turn-around time (on the order of 30-60 min).

This thesis describes the development of such a device based on utilization of an electrochemical Zn sensor developed by Dr. Ian Papautsky and his students<sup>7</sup>.

### **1.3 Research objectives**

Normal Zn homeostasis is critical to a myriad of biological processes that are relevant to critical illnesses<sup>4</sup>, which includes pediatric septic shock. Studies have demonstrated that altered Zn homeostasis is an early and persistent characteristic of pediatric septic shock<sup>1</sup>. A practical and important aspect for Zn supplementation is the ability to allow rapid and direct Point-Of-Care measurement of Zn concentration in blood serum.

The proposed Point-Of-Care device consists of an electrochemical sensor, a potentiostat circuit and a Zinc chip reader. In the proposed device, Zn concentration is measured using Square Wave Anodic Stripping Voltammetry (SWASV). The objective of the potentiostat is to integrate with the sensor and the purpose of Zinc chip reader is to create required environment for conducting SWASV and then to capture and store the data signal generated by the sensor during the SWASV measurement process. The primary focus of this research was to develop a simple, portable and inexpensive instrumentation (Potentiostat and the Zinc chip reader) that can

quantify Zn at the patient's bedside. In addition to providing an accurate method for quantification of Zn in blood serum a primary design objective for the Zn chip reader is to minimize the turn-around time to about an hour. To accomplish the design objectives, the Zn chip reader will be developed using commercially available embedded system components. Figure 1 shows the functional diagram of the Point-Of-Care device.

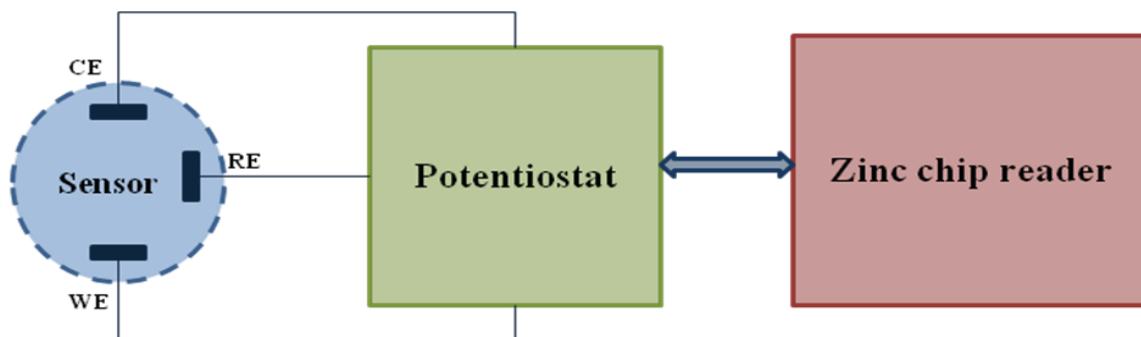


**Figure 1 Functional diagram of the Point-Of-Care system**

## **1.4 Thesis outline**

The next chapter, Chapter 2 – Principles and Design of Instrumentation, discusses the three electrode sensor and the SWSV electroanalytical technique. It also describes the overview of the Zinc chip reader and the potentiostat system design.

Chapter 3 – Development of Instrumentation, describes the design and development of each module of the embedded system.

In Chapter 4 – Experimental Verification, discusses the experimental setup. It also elaborates on the testing procedure and the results will be reported and discussed.

Chapter 5 – Conclusions and Future Work, concludes this research work and also suggests some future work.

## CHAPTER 2

### PRINCIPLES AND DESIGN OF INSTRUMENTATION

#### 2.1 Overview of the three-electrode sensor

The electrochemical sensor was developed by Bio Micro Systems Laboratory at University of Cincinnati, headed by Dr. Ian Papautsky. The sensor is a three electrode system which has a Bismuth(Bi) working electrode, a Ag/AgCl reference electrode and a Gold (Au) auxiliary electrode. Figure 2 shows the electrochemical sensor.

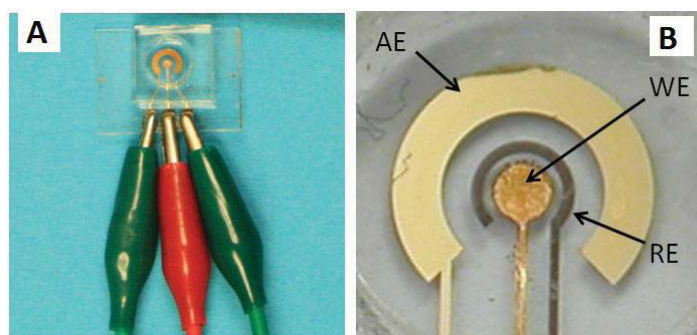


**Figure 2 (A) Photograph of the electrochemical sensor with connectors and (B) close-up image of the sensor electrodes where AE is Gold auxiliary electrode; RE is Ag/AgCl reference electrode; WE is Bi working electrode**

Other electrodes such as hanging drop mercury<sup>8</sup>, mercury thin film<sup>9</sup>, glassy carbon<sup>10</sup> have been reported in literature for the detection of Zn. However, bismuth has become popular recently due to its non-toxic nature, making the sensor convenient for use in point-of-care applications. The sensor was fabricated by means of microfabrication techniques including photolithography, wet-etching, electrodeposition and soft-lithography<sup>7</sup>. Because it provides the lowest detection limits, Anodic Stripping Voltammetry (ASV) is an electroanalytical technique that is widely used for detection of heavy metals in solutions. Of particular interest in this thesis is Square Wave Anodic Stripping Voltammetry (SWASV) which has been used for detection and quantification of Zn. The principles of this electroanalytical technique are discussed in the following section.

## **2.2 Electrochemical detection of Zinc**

### **2.2.1 Overview of Anodic Stripping Voltammetry (ASV)**

ASV is an electroanalytical technique well known for its lowest detection limit and is very commonly used for detection of heavy metals<sup>11</sup>. In its most general form ASV has two steps. In the first step, the analyte in the solution is deposited on an electrode using controlled potential electrolysis. This step serves to preconcentrate the analyte either by electrochemically extracting it as a metal atom into a liquid mercury electrode or depositing it as a metal film on the surface of a solid electrode (Bismuth or Glassy carbon). This Preconcentration phase is responsible for low detection limits. In second step the deposited metal is removed (Stripped) by a potential scan in the anodic direction. The second step will result in a current that is measured and used to quantify the analyte in the sample solution. Since the current generated in the experiment is an anodic current, the name technique is referred to as Anodic stripping voltammetry.

### **2.2.2 Electrochemical sensing of Zinc by Square wave anodic stripping voltammetry**

As described in section 2.2.1 the metal ions are first preconcentrated onto the working electrode and then stripped off during the potential scan. A critically important feature of ASV is that the potential at which each metal strips off is characteristic of that metal. The working potential window for the given electrochemical sensor is -1.6V to -0.3V, this window is limited by the hydrolysis that occurs at voltages below -1.6V and on the other end at -0.3V due to oxidation (stripping) of Bismuth that occurs above this voltage<sup>7</sup>. As shown in Figure 3, Zinc (Zn), Cadmium (Cd) and Lead (Pb) are important metals with stripping potentials in the range



from -1.6V to -0.3V. Thus, Anodic Stripping Voltammetry particularly Square Wave Anodic Stripping Voltammetry (SWASV) is an electroanalytic technique that is well suited for

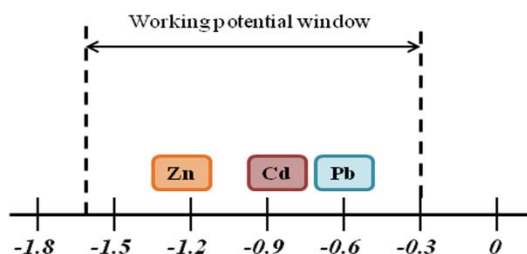


**Figure 3 Stripping potentials of different heavy metals in the working potential window of the sensor**

quantification of Zinc. Quantification is done by measuring the anodic current. The concentration of Zn is proportional to the resultant current. Thus, the exact concentration value can be determined by using a calibration curve.

### **Square Anodic Wave Stripping Voltammetry (SWASV)**

SWASV has three phases as described below:

1. Preconcentration – In the preconcentration phase, the working electrode (WE) is held at a constant potential. During the preconcentration phase,  $\text{Zn}^{+2}$  metal ions are reduced to elemental metal  $\text{Zn}^0$ . As a result, a metallic film is formed over the Bismuth working electrode. It is important to note that during this phase, the sample solution is constantly stirred to ensure that all the metal ions are deposited on the electrode surface.
2. Quiet time – This step is similar to the preconcentration step except that the stirring is turned off. Quiet time allows the system to reach equilibrium.
3. Stripping – In the stripping phase, the deposited metal is stripped off of the electrode surface by applying a stair cased square wave in a positive direction. During the

application of stripping voltage steps, the metal is oxidized back to its ionic form  $\text{Zn}^{+2}$  which generates an anodic current.

Figure 4 illustrates the preconcentration and stripping steps.

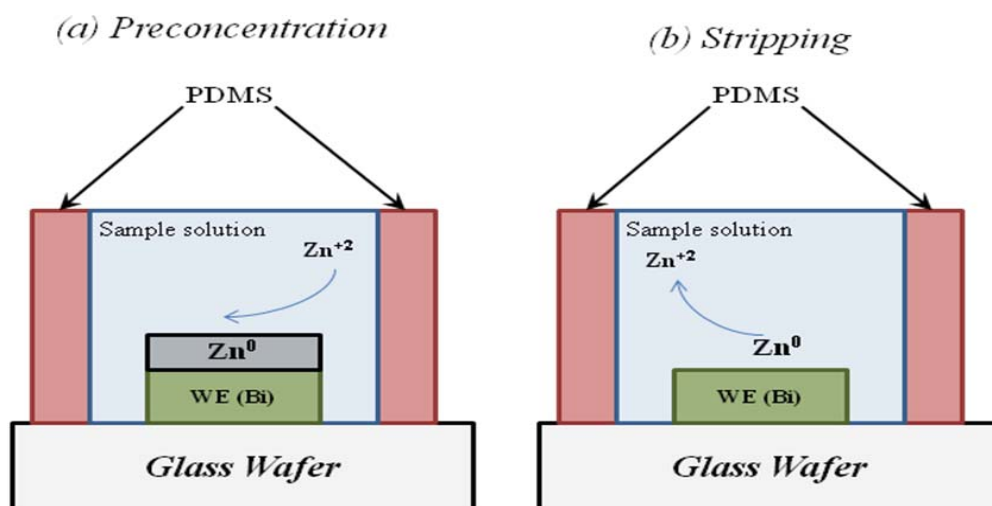


**Figure 4 Square wave anodic stripping voltammetry of Zn on Bi working electrode illustrating the two steps (a) Preconcentration and (b) stripping**

The idea behind square wave stripping voltammetry is that during the stripping phase the excitation signal is a symmetrical square wave signal superimposed on a stair case waveform, where the positive half cycle of the square wave coincides with the step of the stair case pulse<sup>12</sup>.

As shown in Figure 5 the symmetric square wave has an amplitude of  $2E_{\text{sw}}$  and a period of  $T$ , the staircase waveform has a step of  $\Delta E$  and a time period of  $T$  as well. Figure 6 shows the complete potential vs. time waveform of SWASV. Current is measured at the end of each half cycle, difference between the forward and reverse current is plotted against the potential of the staircased waveform. Figure 6 shows the forward current ( $i_f$ ), due to the forward cycle of the square wave, the reverse current ( $i_r$ ) and the net current which is the difference of forward and reverse current. The current measurement window for both forward and reverse pulses is postponed to the end of each pulse to facilitate substantial decay of non-faradic currents. Square

wave voltammetry has several advantages such as minimized interference from non-faradic currents and a fast scanning rate.

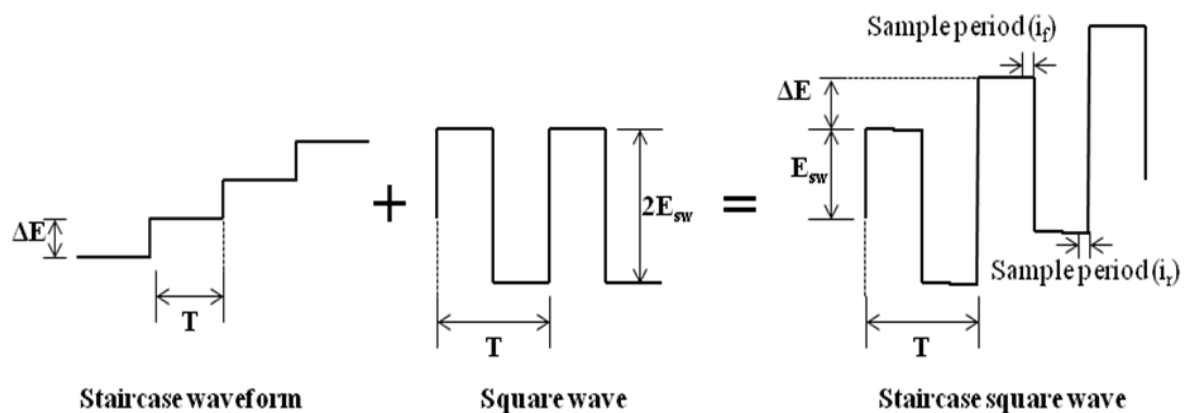


**Figure 5 Square wave superimposed on a staircase waveform**

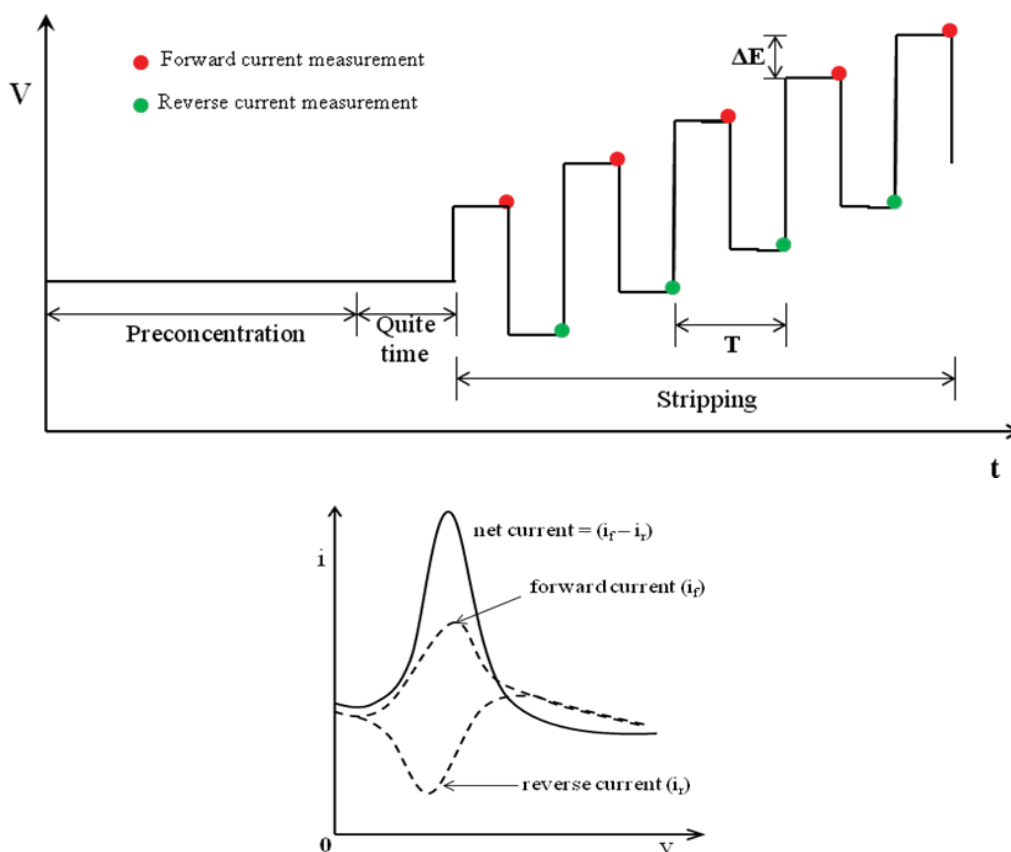


**Figure 6 Excitation signal for square wave stripping voltammetry and the current response signal**

### 2.2.3 The electrochemical sensor and SWASV

The electrochemical sensor has three electrodes the working electrode, reference electrode, counter electrode as shown in Figure 2. The role played by each electrode in ASV is described below

#### **Working Electrode (WE):**

- The required potential is applied at WE in a controlled manner to allow the transfer of analyte ions to and from the sample solution.
- It makes contact with the analyte in the sample solution, i.e. the analyte is deposited on WE during preconcentration phase.
- The anodic current is measured at WE.

#### **Reference Electrode (RE):**

- It is used to measure the cell potential which is used to control the potential at WE.
- No current will be flowing through it.

#### **Counter/Auxiliary electrode (CE):**

- To maintain the cell at a constant potential no current should flow through RE, for this reason a CE is used.
- The purpose of CE is to pass the current needed by WE to balance the system.

The three electrodes sensor along with the potentiostat sets the environment to conduct square wave stripping voltammetry on the sample solution. The hardware system development is discussed in the section below.

## 2.3 Zinc chip reader system design

The zinc chip reader presented in this thesis has been developed to perform two functions. First it is designed to integrate with the sensor for the purpose of providing the required potential profile and measuring the anodic current. Second, the chip reader is designed to provide real time data acquisition and data storage. Figure 7 shows the block diagram of the device. The block diagram of the device instrumentation developed. The Zinc chip reader design centers around an embedded system which dictates the actions of the entire hardware device.

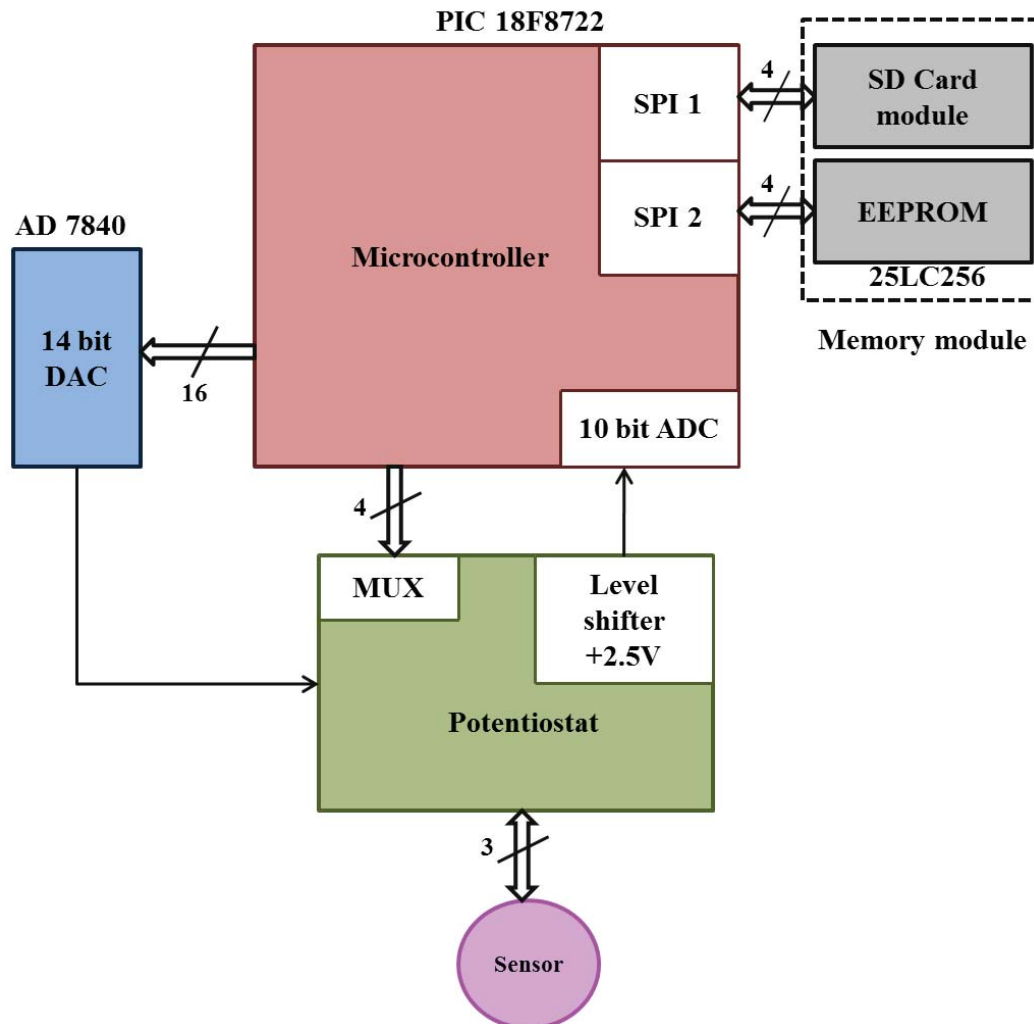


Figure 7 Block diagram of the Zinc chip reader

### 2.3.1 The Embedded System

The embedded system consists of a PICDEM<sup>TM</sup> PIC 18 explorer demonstration board available from Microchip® and other commercially available peripheral devices such as a 14-bit DAC, a 256K byte EEPROM and a SD card module. At the core of the explorer board is a PIC18F8722 microcontroller that is programmed to control and schedule when each section of the hardware is activated. The PIC ports interfaces with the 14 bit DAC which generates the required potential profile for SWASV. The PIC also has an integrated 10 bit Analog to Digital Converter (ADC) module which has been used to digitize the measured current value. Quantification of Zinc is done by measuring the peak current value from an anodic stripping voltammogram, which is plotted as measured current against the input potential. The peak current is compared against a calibration curve to obtain the concentration of Zn. Thus, system operations require storage of the real time data acquired after each half cycle of the stair cased square wave during stripping. . For this purpose an EEPROM has been used to temporarily store data and once the experiment has been completed all the data is transferred to a SD card in a text file format. This enables the data to be transferred to a laptop computer where the voltammogram can be plotted and further analyzed. The PIC accumulates 64 Kbytes (one page of the 25LC256 EEPROM) of this real time data (Voltage and Current) values, acquired during the stripping phase and then schedules the write to EEPROM. After the final stripping phase is completed the PIC and the software are responsible for data transfer onto the SD card. The EEPROM and the SD card are interfaced to the PIC microcontroller using the two Serial Peripheral Interface (SPI) ports available in PIC18F8722. The detailed design and development of each module is discussed in detail in Chapter 3.

### **2.3.2 The Potentiostat**

The potentiostat is a very important electronic circuit responsible for controlling the potential difference between Reference electrode(RE) and working electrode (WE) by sampling the cell potential and varying the Auxiliary Electrode (AE) potential accordingly and it also measures the anodic current from the WE<sup>13</sup>. The detailed design and working of the potentiostat is described in Chapter 3.

## CHAPTER 3

### DEVELOPMENT OF INSTRUMENTATION

The hardware system consists of a zinc chip reader and a potentiostat, which are developed using a PICDEM<sup>TM</sup> PIC 18 explorer demonstration board and other additional peripheral devices. The detailed circuit design of each sub-system is discussed in detail in this chapter. Before that, the following section describes the flow of events for conducting Square Wave Anodic Stripping Voltammetry (SWASV).

#### 3.1 Flow chart for conducting SWASV

Figure 8 shows the flow chart of the events for SWASV. The following steps are involved in implementation of the flow chart.

**Step 1 – Initializing:** First, the following parameters of the input voltage profile are loaded on to the PIC18F8722 microcontroller by changing the values in a program that is compiled and then loaded onto the program memory of PIC18F8722 using the MPLAB® PIC kit 3 programmer:

1. Frequency ( $1/T$ ) in ‘Hz’
2. Step size ( $\Delta E$ ) in ‘mV’
3. Pulse size ( $2E_{SW}$ ) in ‘mV’
4. Preconcentration time in ‘seconds’
5. Quite time in ‘seconds’
6. Initial voltage in ‘V’
7. Final voltage in ‘V’
8. Output file name for the text file on SD card



are taken from the user and loaded on to the PIC18F8722 microcontroller. This will be done by changing the values in the C program and then writing the program onto the program memory of PIC18F8722 using the MPLAB® PIC kit 3 programmer.

**Step 2 – Indicating that the system is ready for SWASV:** Once the input parameter values are loaded all the LED's on the PIC explorer board (Discussed in detail in section 3.2) are turned on to indicate that the set-up is ready to conduct SWASV according to the parameters specified in above step.

**Step 4 – Waiting on button push:** Once the LED's are on the system waits for the button push to trigger the start of the voltammetry process.

**Step 5 – SWASV:** Following the button push the voltammetry process begins (Preconcentration → quite time → stripping). Concurrently the forward and reverse current readings are taken and stored into the EEPROM along with the corresponding input voltage value. All the values are stored in ASCII format. Figure 9 shows the flow chart for each cycle of the stripping phase.

**Step 6 – Moving data from EEPROM to SD card:** After the SWASV has completed the experimental data that has been stored in the EEPROM is transferred to the SD card as a text file in a directory by the name that has been specified as an input in step 1.

**Step 7 – Analyzing data:**

Now that the data is on a SD card it can be loaded onto a computer, plotted and analyzed using a data processor software such as MATLAB®, Microsoft Excel ® etc. The peak current should be measured and Zn concentration is quantified using this current value and the calibration curve.

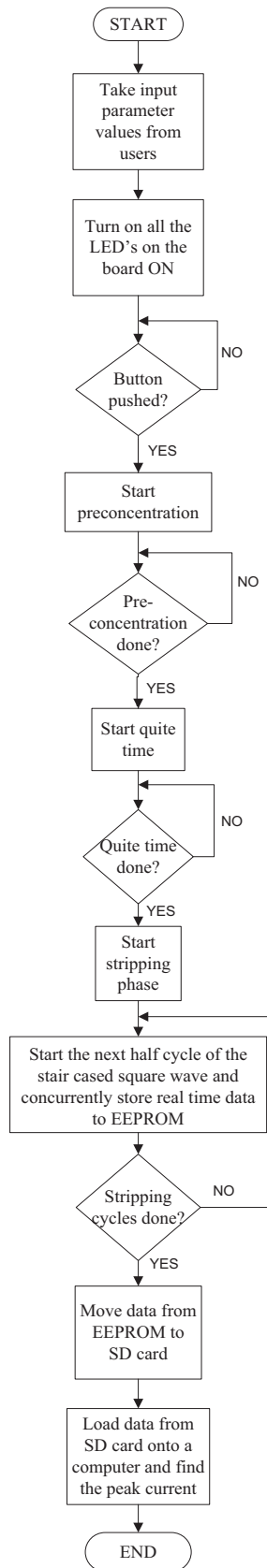


**Figure 8 Flow chart for conducting SWASV**

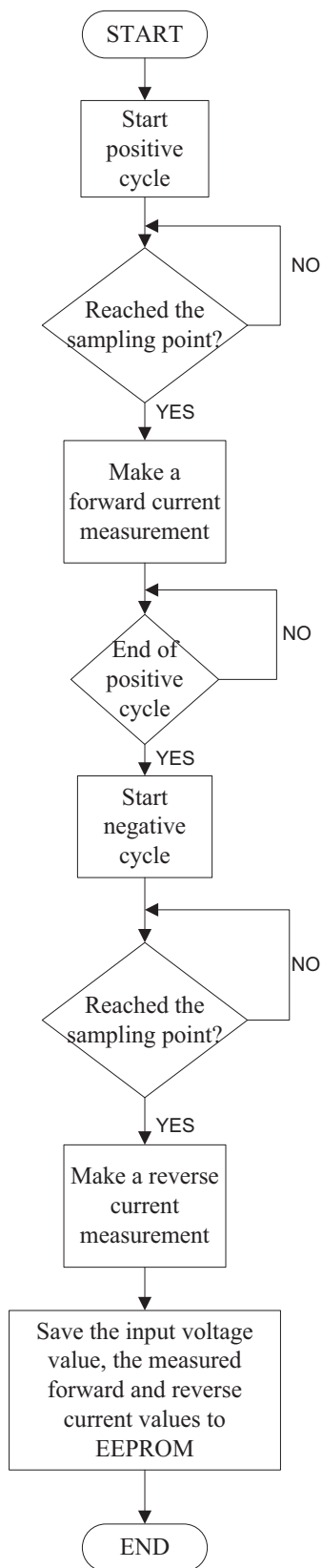


**Figure 9 Flow chart showing the steps involved in each cycle of the stripping phase**

### 3.2 The PICDEM™ PIC 18 explorer demonstration board

The entire zinc chip reader has been developed around a PICDEM™ PIC 18 explorer demonstration board containing a PIC18F8722 microcontroller. Figure 10<sup>14</sup> shows the explorer board with all its hardware components numbered and only those components that are being used in this research are marked with red boxes. And Figure 11<sup>14</sup> lists all the hardware components present on the explorer board, again only those components that are relevant to this research

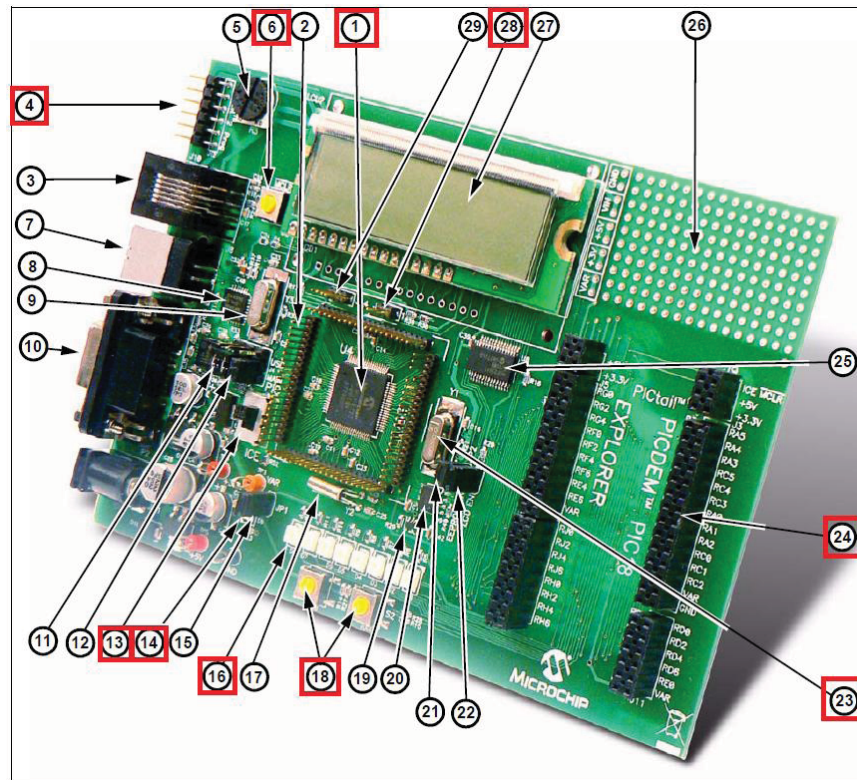


**Figure 10 Picture of PICDEM™ PIC 18 explorer demonstration board<sup>14</sup>**

work are highlighted in red boxes. The numbers in Figure 10 and Figure 11 are consistent with respect to each other. The required software to control all the events for the Point-Of-Care device is loaded onto the PIC18F8722 microcontroller through the six - pin PICKit™ 3 programmer that interfaces with MPLAB® IDE (Integrated development environment) hence this board is the control unit for the entire system. The development board has many features and

hardware components designed by Microchip® for developing general purpose applications. But, only few of those features and components have been used in developing the Zinc chip reader instrumentation.

The PICDEM PIC18 Explorer Demonstration Board has the following hardware features with each feature's number corresponding to the number in Figure that shows the feature's location on the board:

1. PIC18F8722 microcontroller – The sample, primary microcontroller mounted on the board.
2. Male header pins for connecting Plug-In Modules (PIMs). A PIM enables an alternate PIC18 device to be connected to the board, as the primary microcontroller.
3. In-Circuit Debugger (ICD) connector.
4. Six-pin, PICKIT™ 3 connector.
5. 10 kΩ potentiometer for analog inputs.
6. Push button switch – For external Reset.
7. USB connector – For RS-232 communication.
8. PIC18LF2450 microcontroller – For converting RS-232 communication to USB protocol for attachment of a host PC.
9. 12 MHz crystal – For the PIC18LF2450 microcontroller.
10. RS-232 DB9 socket and associated hardware – For direct connection to an RS-232 interface.
11. Jumper J13 for routing RS-232 communication through either the USB port or the RS-232 socket.
12. Jumper J4 – For selecting between programming the main PIC® device or the PIC18LF2450, used for USB to RS-232 communication.
13. Switch S4 – For designating the main microcontroller as either the board-mounted PIC18F8722 or a PIM-mounted microcontroller.
14. LED – For power-on indication.
15. JP1 – For disconnecting the eight display LEDs.
16. Eight LEDs.
17. 32.768 kHz crystal – For Timer1 clock operation.
18. Two push button switches – For external stimulus.
19. Analog temperature sensor, MPC9701A.
20. 25LC256 SPI EEPROM.
21. JP2 – To enable/disable EEPROM.
22. JP3 – To enable/disable LCD.
23. 10 MHz crystal – For the main microcontroller.
24. PICTail™ daughter board connector socket.
25. SPI I/O expander – For LCD display, MCP23S17.
26. Prototype area – For user hardware.
27. LCD display.
28. J2 three-pin, male header – For selecting between a voltage of 3.3V or 5V.
29. J14 four-pin, male header – For use with a PIM, if required, to connect 3.3V or 5V, VIN and ICE MCLR.

**Figure 11 List of components of the PICDEM™ PIC 18 explorer demonstration board<sup>14</sup>**

Following are the components that are used in the application development

1. PIC18F8722 microcontroller – mounted on the explorer board (will be discussed in detail in the section 3.3)
4. six- pin PICKit™ 3 connector – that connects the board to a PICKit™ 3 programmer which in turn interacts with the MPLAB® IDE for downloading the software C program onto the PIC.
6. Push buttons for external reset – when this button is pushed the microcontroller is reset, and this has been disabled in software to avoid any accidental use while the experiment is running.
13. Switch S4 – the explorer board also supports a PIM (Plug In Module) where we can plug in other compatible microcontroller, this switch S4 is used to select between onboard PIC18F8722 or PIM. For our application we are using the onboard PIC18F8722 hence the switch is positioned accordingly.
14. LED – indicates if the explorer board is powered up.
16. Eight display LED's – These LED's are connected to a port of the Microcontroller and are being used to indicate the state of the system.
18. Two push buttons (S0, S1) – one of these push buttons S0 has been programmed to trigger the start of voltammetry process.
23. 10MHz crystal – this provides the clock for the microcontroller.
24. PICtail™ connector socket – this connector socket has been used to connect the PCB which was designed to host all the peripheral devices and the potentiostat circuit.
28. J2 three pin male header – the board can supply 5V or 3.3V depending on the voltage level for the microcontroller. PIC18F8722 has 5V logic levels hence J2 is configured to supply 5V.

### 3.3 Programming the microcontroller

The explorer board can be configured in 3 different modes – stand alone board, with in circuit debugger or with a PIM. Table 1<sup>14</sup> summarizes the three modes and their configuration.

**Table 1 Different configurations of PICDEM™ PIC 18 explorer demonstration board<sup>14</sup>**

Configuration	Board Connections	Board Capabilities
Stand-alone board	Power supply	<ul style="list-style-type: none"><li>• Access board's full functionality</li><li>• Demonstrate sample code</li><li>• Display functionality with LCD or LEDs</li><li>• Connect ICD/programmer for debugging or programming</li><li>• Connect PICTail™ daughter cards</li></ul>
Board with in-circuit debugger/programmer	<ul style="list-style-type: none"><li>• Power supply</li><li>• In-Circuit Debugger (ICD) that also can be used as a programmer</li></ul>	<ul style="list-style-type: none"><li>• Access board's full functionality</li><li>• Demonstrate sample code</li><li>• Develop and debug code</li><li>• Reprogram microcontrollers</li><li>• Connect PICTail daughter cards</li></ul>
Board with alternate microcontroller, attached through a Plug-In Module (PIM)	<ul style="list-style-type: none"><li>• Power supply</li><li>• ICD that also can be used as a programmer</li><li>• PIM with mounted microcontroller</li></ul>	<ul style="list-style-type: none"><li>• Substitute PIM-mounted device as main microcontroller†</li><li>• Use 3.3V or 5V devices as main microcontroller</li><li>• Demonstrate sample code</li><li>• Develop and debug code</li><li>• Reprogram microcontrollers</li><li>• Connect PICTail daughter cards</li></ul>

For our application the board works in a stand-alone mode powered from a wall socket with the required software already programmed onto the microcontroller. But during the developmental stages the board was used with in-circuit debugger mode to detect and correct errors. This board can perform all the required functionality for the Zinc chip reader. Its expansion port (PICTail™ connector socket) provides very good connection for the PCB board. This board also has enough functionality for expanding the display and data entry modules in future, using the LCD, push buttons and the potentiometer.

To program the device the source code (written in C) is compiled using the MPLAB C18® compiler which generates a HEX file. The PICkit 3 programmer is then used to program the flash memory on the microcontroller with the generated HEX code.

### **3.4 The PIC18F8722 microcontroller**

A software program has been developed to schedule and control when each section of the hardware is activated. These commands from the software are used by the microcontroller to digitally control various peripheral devices that are connected to the I/O ports of the microcontroller. The software is stored in the program memory of the microcontroller. Thus the microcontroller is responsible for all the flow of events as shown in flow charts of Figure 8 and Figure 9. All the above actions are performed by the PIC18F8722 microcontroller that is mounted on the PIC 18 explorer board.

#### **3.4.1 Peripheral highlights and features**

PIC18F8722 is an 80 Pin 1 Mbit enhanced flash microcontroller with the following special features and highlights<sup>15</sup>

##### **Peripheral and memory highlights:**

- 70 I/O port pins
- 16 channel, 10 bit Analog to Digital Converter (ADC) with auto acquisition capability.
- 4 programmable external interrupts
- 4 input change interrupts
- 2 Serial Peripheral Interface (SPI) ports
- Address capability upto 2Mbits with external memory addressing
- Flexible 8, 12, 16 or 20 bit addressing modes
- 128K bytes flash memory and substantial data memory with 3936 Bytes SRAM and 1024 Bytes internal EEPROM



Special features:

- C compiler optimized architecture
- In-circuit debugger
- Two 8-bit timers and three 16-bit timers and up to 10 different oscillator options
- nanoWatt technology – new core technology that can significantly reduce power consumption

### 3.4.2 Pin description

PIC18F8722 has 80 pins, Figure 12<sup>15</sup> shows the pin diagram along with the color coding, which specifies connections to the corresponding peripheral devices. And the Table 2 gives the pin description of only those pins that are being used. The entire pin description can be found in PIC18F8722 family datasheet<sup>15</sup>.

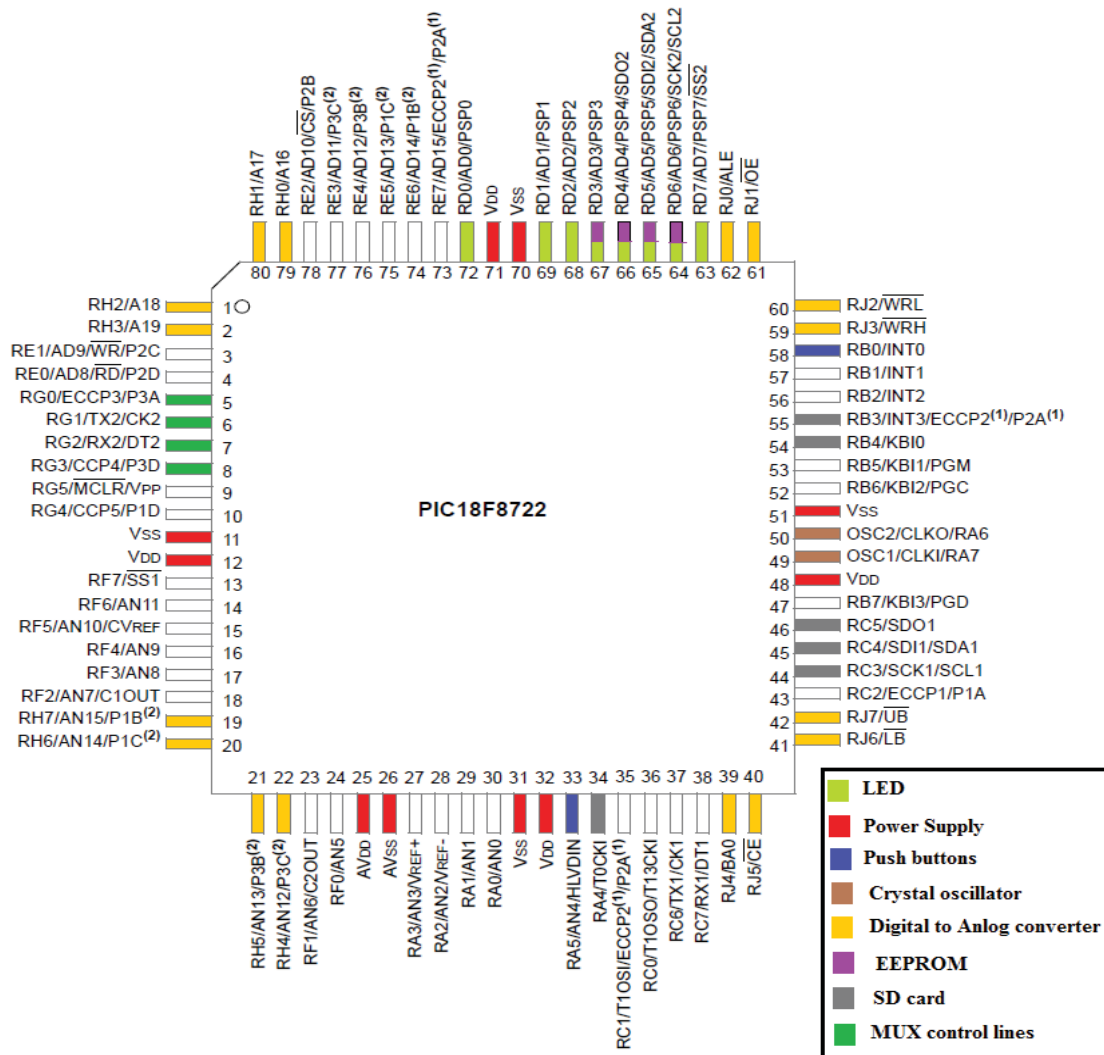
#### I/O ports:

There are 70 I/O pins divided as nine ports – A, B, C, D, E, F, G, H, and J. Each of which are bidirectional and 8-bit wide except for Port G which is only 6-bit wide. These I/O pins are multiplexed with an alternative functionality (peripheral features of the device). These pins cannot be used as general purpose I/O when the peripheral feature is being used.

Each port has three registers associated with them

1. **PORT** register – reads the levels on the associated pins. Ex: PORTA register will read the status of PORTA pins and this value can be used later in the program by copying to a variable.

2. **TRIS** register – data direction register, used to make a particular pin input (=1) or output (=0). Ex: making a bit in PORTA equal to 1 will make it an input pin.
3. **LAT** register – the data latch register used for read-modify write. Ex: LATA will write the value assigned to it on to the corresponding port pins



Note 1: The ECCP2/P2A pin placement is determined by the CCP2MX configuration bit and Processor mode settings.  
 Note 2: P1B, P1C, P3B and P3C pin placement is determined by the ECCPMX configuration bit.

**Figure 12 Pin diagram of PIC18F8722 and the color coding indicates the connections to various peripheral devices<sup>15</sup>**

**Table 2 Pin description of PIC18F8722 (only those that are used)**

Pin Name	Function	I/O	Description
OSC2/CLK0/RA6	OSC2	O	10MHz crystal oscillator feedback output connection
OSC1/CLK1/RA7	OSC1	I	10MHz crystal oscillator input connection
RB0/INT0/FLT0	INT0	I	External interrupt 0 connected to the switch S0
RC3/SCK1/SCL1	SCK1	O	SPI 1 module clock output connected to SD card
RC4/SDI1/SDA1	SDI1	I	SPI 1 data input connected to data O/P of the SD card
RC5/SDO1	SDO1	O	SPI1 data output connected to data I/P of the SD card
RD0 – RD7*	RD0 – RD7	O	Used as data output port connected to the 8 LED's on board.
RD4/AD4/ PSP4/SDO2*	SDO2	O	SPI 2 data output connected to data I/P of the EEPROM
RD5/AD5/ PSP5/SDA2*	SDI2	I	SPI 2 data input connected to data O/P of the EEPROM
RD6/AD6/ PSP6/SCK2/SCL2*	SCK2	I	SPI 2 module clock output connected to EEPROM
RF3/AN8	AN8	I	A/D input channel 8 connected to +5V power supply to make a full scale reading.
RF4/AN9	AN9	I	A/D input channel 9 connected to the output of level shifter of the potentiostat board
RG0/ECCP3/P3A	RG0	O	Data output pin connected to A0 select line of the 8X1 MUX
RG1/TX2/CK2	RG1	O	Data output pin connected to A1 select line of the 8X1 MUX
RG2/RX2/DT2	RG2	O	Data output pin connected to A3 select line of the 8X1 MUX
RG3/CCP4/P3D	RG3	O	Data output pin connected Enable of the 8X1 MUX
RG5/MCLR/VPP	MCLR	I	External memory clear input pin, it is disabled by clearing the MCLR configuration bit
RH0 –RH7	RH0 – RH7	O	Connected to the data in lines of the Digital to Analog converter.
RJ0 –RJ7	RJ0 –RJ7		Connected to the data in ands the control lines of the Digital to Analog converter.

Note 1: Few pins in PORTD are multiplexed between the LED's and the EEPROM, The SPI mode has a priority over data out.

### 3.4.3 Interrupts

PIC18F8722 has several interrupt sources both external and internal. And it also has priority levels for the interrupts, the high priority interrupt vectors are at 0008h and the lower priority interrupt vectors are defined at 0018h. However if not needed these priority levels can be disabled in software. Different registers are used to control the interrupt operation (RCON, INTCON, INTCON2, INTCON3, PIR1, PIR2, PIR3, PIE1, PIE2, PIE3, IPR1, IPR2, IPR3)<sup>15</sup>. In general the interrupts have 3 bits to control their operations

1. **Priority bit:** Used to set the priority levels on the interrupt source.
2. **Enable bit:** the program branches to the interrupt vector only when the corresponding enable bit for the interrupt source is set.
3. **Flag bit:** when an interrupt occurs this bit will be set.

**Ex:** To use the interrupt on timer 0 overflow we first have to enable the interrupt by setting the corresponding interrupt enable bit, `INTCONbits.TMR0IE = 1;`

Only then the program will move to Interrupt Service Routine (ISR) when the Timer 0 overflows, `INTCONbits.TMR0IF = 1` (interrupt flag bit is set);

### 3.4.4 Oscillators and timers

#### Oscillators and clock sources:

PIC18F8722 has three clock sources, Primary, secondary and internal oscillators. This device has a feature that the clock source can be switched. The three sources are briefed below:

1. *Primary oscillator:* from external crystal connected between OSC1 and OSC2 pins. For the explorer board we have a 10MHz crystal oscillator connected between these pins.

2. *Secondary oscillator:* is also an external oscillator source but connected between T1OSI and T1OSO pins, most often a 32.768KHz crystal is connected between them. These sources continue to operate even in power management mode. Ex: Timer 1 oscillator could be used as secondary source, as it operated even in power management mode it can be used as time base for real time clock.
3. *Internal oscillator:* The main output of the internal oscillator is an 8MHz clock which can drive the device directly or a postscaler can be used to generate clock frequencies in the range of 31KHz to 4MHz.

Figure 13<sup>15</sup> shows the different clock sources for PIC18F8722, and the modules that are used are marked in red. In our application development we have used the 8MHz internal oscillator and then used a 4 X PLL to generate a 32MHz clock for the system. The PLL is discussed below.

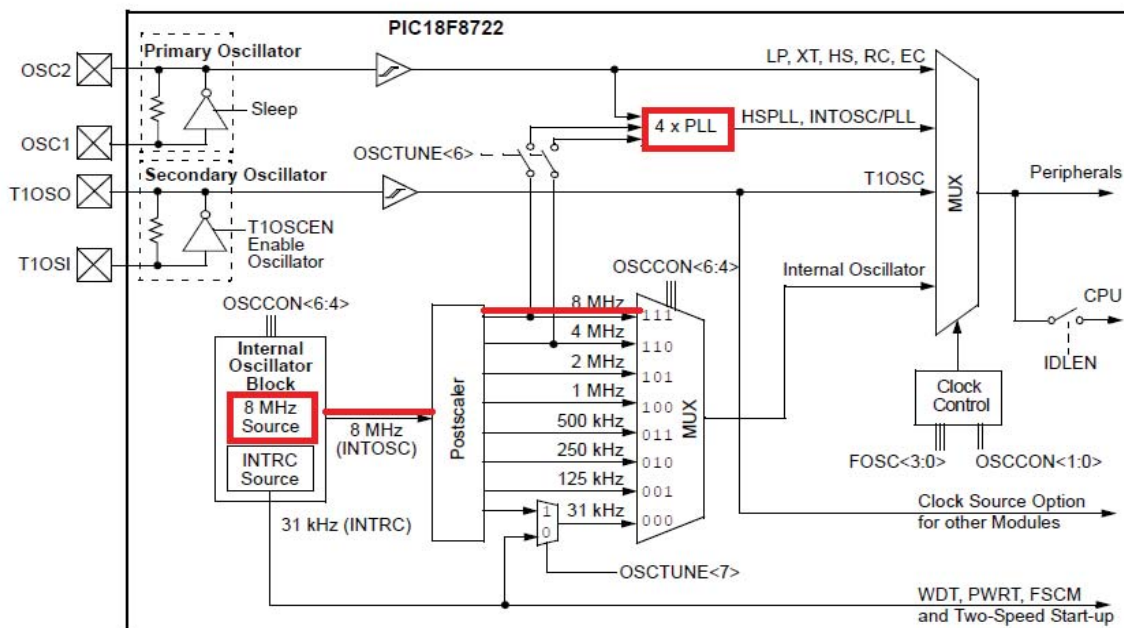


Figure 13 PIC18F8722 clock sources and oscillator switching<sup>15</sup>

### Internal oscillator and PLL:

The PIC18F8722 can be operated in 10 different modes and Table 3<sup>15</sup> summarized these different modes. The oscillator for our application has been configured in INTIO2 mode. Also the PLL is used to produce faster device clocks (32MHz) using the internal oscillator and this is

**Table 3 PIC18F8722 oscillator modes<sup>15</sup>**

	Mode	Description
1.	LP	Low-Power Crystal
2.	XT	Crystal/Resonator
3.	HS	High-Speed Crystal/Resonator
4.	HSPLL	High-Speed Crystal/Resonator with PLL enabled
5.	RC	External Resistor/Capacitor with Fosc/4 output on RA6
6.	RCIO	External Resistor/Capacitor with I/O on RA6
7.	INTIO1	Internal Oscillator with Fosc/4 output on RA6 and I/O on RA7
8.	INTIO2	Internal Oscillator with I/O on RA6 and RA7
9.	EC	External Clock with Fosc/4 output
10.	ECIO	External Clock with I/O on RA6

all controlled by the software.

### 3.4.5 10-Bit Analog to Digital Converter (ADC) module

PIC18F8722 has an integrated 10-Bit ADC with 16 channels which allows converting the analog input signal into a corresponding 10-bit digital number. An ADC is required to digitize the analog output signal from the potentiostat and this integrated 10-bit ADC is being used to digitize the analog output values. The ADC module will be discussed in detail as it has been used extensively. The potentiostat analog output is connected to channel AN9 of the ADC. Figure 14<sup>15</sup> shows the block diagram of the ADC module.



ADCON0, shown in Figure 15, controls the operations of ADC module by enabling the module, selecting the channel and it also indicated the conversion status. ADCON1, shown in Figure 15, configures the port functioning and sets the voltage reference for conversion. ADCON2, shown in Figure 16, is used to configure the clock source and acquisition time for ADC conversion, to select the justification of the result. Since the result of a conversion is a 10-bit value it cannot be stored in one register; hence two registers ADRESH: ADRESL together hold the results. Depending on the left/ right justification specified one register holds 8 bits and the other holds the remaining two bits.

<b>Legend:</b>			
R = Readable bit	W = Writable bit	U = Unimplemented bit, read as '0'	
-n = Value at POR	'1' = Bit is set	'0' = Bit is cleared	x = Bit is unknown

ADCON0: A/D CONTROL REGISTER							
U-0	U-0	R/W-0	R/W-0	R/W-0	R/W-0	R/W-0	R/W-0
—	—	CHS3	CHS2	CHS1 <sup>(1)</sup>	CHS0 <sup>(1)</sup>	GO/DONE	ADON
bit 7				bit 0			

bit 7-6	<b>Unimplemented:</b> Read as '0'
bit 5-2	<b>CHS&lt;3:0&gt;</b> Analog Channel Select bits <div>             0000 = Channel 0 (AN0)              0001 = Channel 1 (AN1)              0010 = Channel 2 (AN2)              0011 = Channel 3 (AN3)              0100 = Channel 4 (AN4)              0101 = Channel 5 (AN5)              0110 = Channel 6 (AN6)              0111 = Channel 7 (AN7)              1000 = Channel 8 (AN8)              1001 = Channel 9 (AN9)              1010 = Channel 10 (AN10)              1011 = Channel 11 (AN11)              1100 = Channel 12 (AN12)              1101 = Channel 13 (AN13)              1110 = Channel 14 (AN14)              1111 = Channel 15 (AN15)           </div>
bit 1	<b>GO/DONE:</b> A/D Conversion Status bit When <b>ADON = 1</b> : 1 = A/D conversion in progress 0 = A/D Idle
bit 0	<b>ADON:</b> A/D On bit 1 = A/D converter module is enabled 0 = A/D converter module is disabled

ADCON1: A/D CONTROL REGISTER 1							
U-0	U-0	R/W-0	R/W-0	R/W-0	R/W-0	R/W-0	R/W-0
—	—	VCFG1	VCFG0	PCFG3	PCFG2	PCFG1	PCFG0
bit 7				bit 0			

bit 7-6	<b>Unimplemented:</b> Read as '0'															
bit 5-4	<b>VCFG&lt;1:0&gt;</b> : Voltage Reference Configuration bits <table> <tr> <th></th><th>A/D VREF+</th><th>A/D VREF-</th></tr> <tr> <td>00</td><td>AVDD</td><td>AVSS</td></tr> <tr> <td>01</td><td>External VREF+</td><td>AVSS</td></tr> <tr> <td>10</td><td>AVDD</td><td>External VREF-</td></tr> <tr> <td>11</td><td>External VREF+</td><td>External VREF-</td></tr> </table>		A/D VREF+	A/D VREF-	00	AVDD	AVSS	01	External VREF+	AVSS	10	AVDD	External VREF-	11	External VREF+	External VREF-
	A/D VREF+	A/D VREF-														
00	AVDD	AVSS														
01	External VREF+	AVSS														
10	AVDD	External VREF-														
11	External VREF+	External VREF-														
bit 3-0	<b>PCFG&lt;3:0&gt;</b> : A/D Port Configuration Control bits:															



#### ADCON2: A/D CONTROL REGISTER 2

R/W-0	U-0	R/W-0	R/W-0	R/W-0	R/W-0	R/W-0	R/W-0
ADFM	—	ACQT2	ACQT1	ACQT0	ADCS2	ADCS1	ADCS0
bit 7							bit 0

bit 7	<b>ADFM:</b> A/D Result Format Select bit 1 = Right justified 0 = Left justified
bit 6	<b>Unimplemented:</b> Read as '0'
bit 5-3	<b>ACQT&lt;2:0&gt;:</b> A/D Acquisition Time Select bits 111 = 20 TAD 110 = 16 TAD 101 = 12 TAD 100 = 8 TAD 011 = 6 TAD 010 = 4 TAD 001 = 2 TAD 000 = 0 TAD <sup>(1)</sup>
bit 2-0	<b>ADCS&lt;2:0&gt;:</b> A/D Conversion Clock Select bits 111 = FRC (clock derived from A/D RC oscillator) 110 = Fosc/64 101 = Fosc/16 100 = Fosc/4 011 = FRC (clock derived from A/D RC oscillator) 010 = Fosc/32 001 = Fosc/8 000 = Fosc/2

**Figure 16 Configuration of ADCON2 register of the ADC module<sup>15</sup>**

#### ADC reference voltage settings:

The analog reference voltage used by the ADC can be programmed in software either as the device's positive or negative supply voltages or to use external reference voltage on Vref+ and Vref- pins. ADC has a 10-bit resolution meaning that input voltage (Vin) range of 0V – 5V is represented by the numbers 0 – 1023. In mathematical terms

$$ADCvalue = \left( \frac{V_{in}}{V_{ref}} \right) \times 1023 \quad (1)$$

In our project we have used the devices supply voltages as reference, hence Vref = 5V. Given the 10 bit ADC value it can be converted back to the analog input voltage value as follows

$$V_{in} = \frac{ADCvalue \times 5}{1023} \quad (2)$$

### Selecting acquisition time and conversion clock:

There is a holding capacitor that must be allowed to charge to the applied input channel voltage, because the capacitor will be disconnected from the input pin when the conversion is started. For accurate operation of the ADC module the acquisition time must be greater than the minimum acquisition time specified in the data sheet as parameter 132<sup>15</sup>. From the PIC18F8722 data sheet<sup>15</sup>  $T_{ACQ}$  is 1.4 $\mu$ s. Here the input to the ADC module comes from a RC network which has a long settling time hence we choose the longest available acquisition time of  $20T_{AD}$ , i.e. 20 times the ADC clock period.

The ADC clock period should be as small as possible at the same time it must be greater than the minimum period  $T_{AD}$  specified as parameter 130 in the data sheet<sup>15</sup>. The minimum  $T_{AD}$  for PIC18F8722 is 1 $\mu$ s. At 32MHz frequency if we pick the ADC clock frequency as  $F_{OSC}/64$  (32MHz/2 = 500KHz), One clock period would be 2 $\mu$ s (1/500KHz) which is greater than the minimum  $T_{AD}$  (1 $\mu$ s).

The ADCON2 register is configured to reflect the acquisition time of  $20T_{AD}$  and a conversion clock period of  $F_{OSC}/64$ .

### Steps to be followed for an ADC conversion:

1. Configure the ADC settings using ADCON0, ADCON1, ADCON2 to reflect the selected input channel, reference voltages, result justification, acquisition time and clock period.
2. Declare the corresponding ADC channel as an input pin.
3. Enable the ADC module by setting ADCON0bits.ADON
4. Start the ADC conversion

5. Wait for the conversion to complete. This can be done by either polling for GO/DONE bit or waiting for the ADC interrupt (if enabled).
6. Read the ADC result register ADRESH:ADRESL and clear the interrupt flag (if used).
7. Use equation (2) to convert back the 10-bit value to an analog voltage value.

### **3.4.6 MSSP module and SPI**

PIC18F8722 has a Master Synchronous Serial Port (MSSP) module to communicate with other peripheral devices such as serial EEPROMs, external serial ADC's or display drivers. MSSP can operate in two different modes:

1. Serial Peripheral interface (SPI)
2. Inter integrated Circuits (I<sup>2</sup>C<sup>TM</sup>)

In the memory module of the Zinc chip reader we have used a serial EEPROM (25LC256) and a SD card each of which communicate with the microcontroller using the SPI mode.

#### **SPI Mode**

8-bits of data can be synchronously transmitted / received simultaneously using the SPI mode. The SPI module can be connected either in a master mode or a slave mode. PIC18F8722 has two SPI modules SPI1 and SPI2. For communication each SPI module uses three pins<sup>15</sup>

1. Serial data out (SDO1, SDO2)
2. Serial data in (SDI1, SDI2)
3. Serial clock (SCK1, SCK2)

In slave mode there is another additional pin slave select. SPI module uses four registers which include a status register (SSP1STAT, SSP2STAT), a control registers (SSP1CON1, SSP2CON1), a serial receive/transmit buffer register (SSP1BUF, SSP2BUF) and a shift register (SSP1SR, SSP2SR). The shift register cannot be accessed directly, in receive mode the data is first loaded bit by bit into the shift register and once all the 8-bits are loaded it will be transferred to the SSPxBUF buffer register, the interrupt flag is set whereas in transmit mode data is written to both the shift register and the buffer register.

The device can be used as a master or a slave,

- In master mode the device provide the serial clock SCKx, and it determines when the connected slave device should transmit its data using the software protocol.
- In slave mode serial clock is supplied by and external master onto the SCKx pin and data will be transmitted/received depending on the arrival of the serial clock.

In our design the microcontroller is the master and the memory devices (serial EEPROM and the SD card) are configured as slaves. Figure 17<sup>15</sup> shows the master – slave connection between the devices. Detailed configuration of the two SPI modes (SPI1, SPI2) will be discussed in section 3.

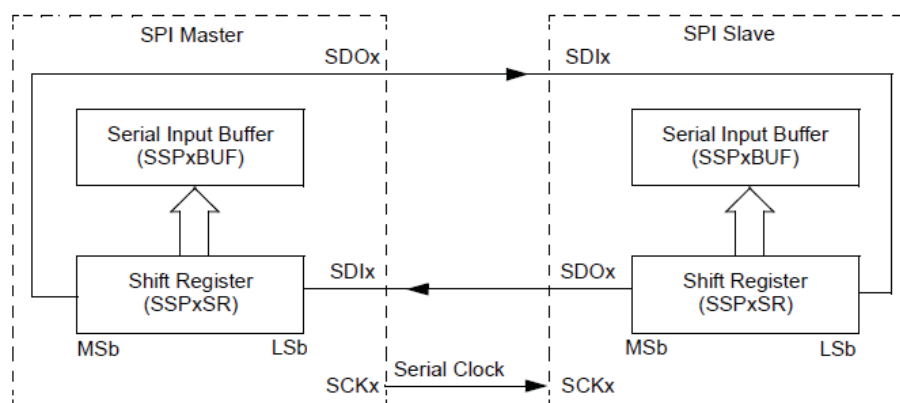


**Figure 17 Master - Slave connection in SPI mode<sup>15</sup>**

### 3.5 The Digital to Analog converter module

The microcontroller can output only digital voltages with low (0V) or high (5V) output. Hence a Digital to Analog Converter (DAC) will be required to generate the required input voltage profile for SWASV. For this purpose a DAC module has been developed using a commercially available 14-bit DAC – AD7840 from Analog Devices®.

AD7840 is a 14 bit DAC with the following features<sup>16</sup>

- Bipolar analog output of  $\pm 3V$
- Parallel and serial interface capabilities
- Provides a very fast interface in parallel mode with a data setup time of 21ns.
- Low Signal – Noise Ratio
- Double buffering interface: 14-bit input latch and 14-bit DAC latch. Data is first loaded

onto the input latch and then transferred to DAC latch under the control of  $\overline{LDAC}$  signal.

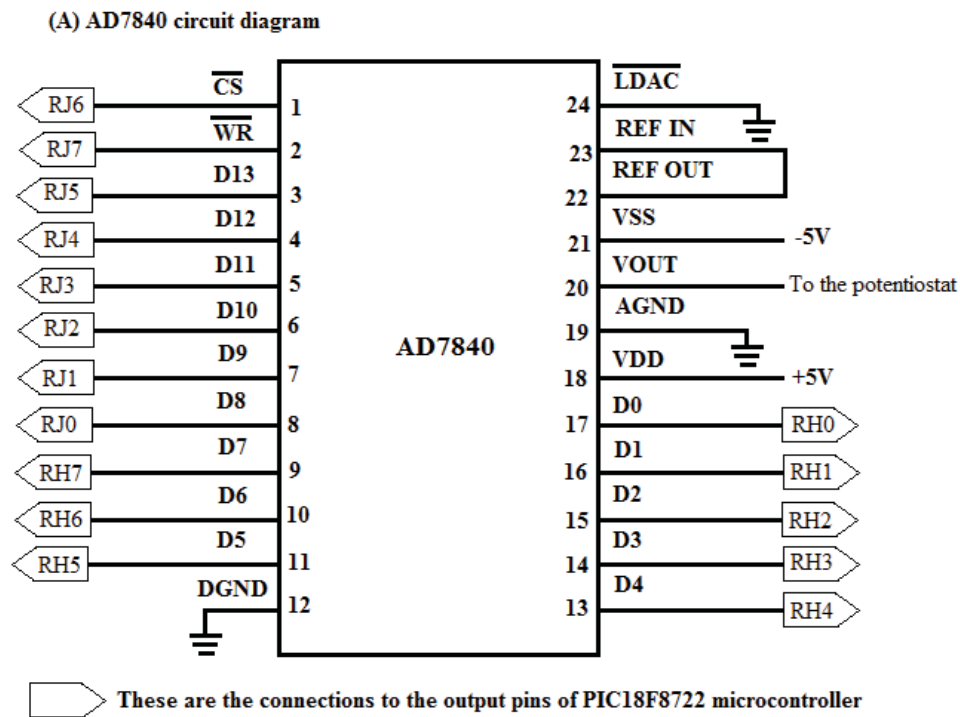
The DAC is operated in parallel mode in our application. In parallel mode the 14-bit input data appearing on the data lines D13 (MSB) to D0 (LSB) is loaded onto the input latch at the same time. The control signals  $\overline{CS}$  and  $\overline{WR}$ , control the above operation. These signals are level triggered when both the signals are held low the input latch becomes transparent i.e. the input data is loaded onto the input latch. DAC latch is level triggered as well and is controlled by  $\overline{LDAC}$ . But both the latches should not become transparent at the same time, to avoid this condition  $\overline{LDAC}$  is hardwired to ground. With  $\overline{LDAC}$  hardwired to ground DAC latch is transparent when  $\overline{CS}$  and  $\overline{WR}$  are high and input latch is transparent when  $\overline{CS}$  and  $\overline{WR}$  are low. Figure 18(B)<sup>16</sup> shows the timing diagram for the procedure discussed above. The circuit connections for the AD7840 DAC are shown in Figure 18(A), the 14 data lines of AD7840 are

connected to pins H0 – H1 and pins J0 – J5 of the PIC and the control signals  $\overline{CS}$  and  $\overline{WR}$  are connected to J6, J7 pins.

Output voltage in terms of the 14-bit input is expressed as follows

$$V_{out} = \frac{2 \times N \times REF_{IN}}{16384}; -8192 \leq N \leq +8191 \quad (3)$$

Where N is the 14-bit value.



(B) Parallel mode timing diagram

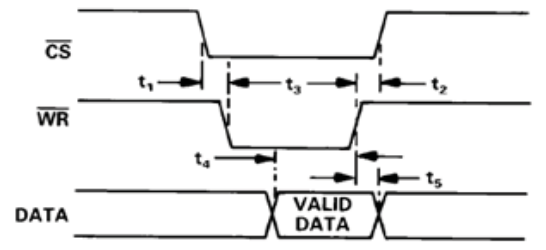


Figure 18 (A) Circuit diagram of 14-bit DAC (AD7840), (B) Parallel mode timing diagram<sup>16</sup>

In SWASV after each cycle a new 14 bit value corresponding to the next cycle voltage is computed by the PIC18F8722 microcontroller using the above equation and is loaded onto the DAC to be converted to the analog voltage. The positive power supply  $V_{DD}$  is derived from the PIC 18 explorer board and the negative power supply  $V_{SS}$  is derived from a -5V supply mounted on the PCB board designed.

### 3.6 Construction of the potentiostat

Potentiostat is a very important circuit that controls the three electrode sensor and interfaces it with the rest of the hardware. It is primarily responsible for performing the following three functions

1. Sample the cell potential using a Reference Electrode (RE)
2. Maintain the required potential difference between the Working and the reference electrodes, using the sampled voltage.
3. Measure the anodic current at the working electrode

A typical potentiostat is constructed using operational amplifiers to perform all the three tasks listed above. Following section gives an overview of different operational amplifier configurations used to build the potentiostat.

#### 3.6.1 Overview of operational amplifier configurations

An operational amplifier has two inputs – inverting input (-) and non-inverting input (+) and one output terminal, see Figure 19. The basic property of operational amplifiers is that it inverts, amplifies the difference between the two input terminals ( $V_{diff}$ ), which is given by the following equation.

$$V_{out} = -A \times V_{diff} \quad (4)$$

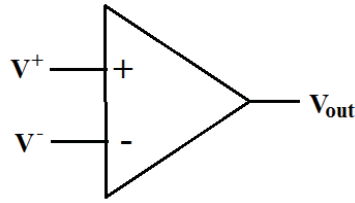


**Figure 19 An operational amplifier**

Where,  $A$  is called the open loop gains, open loop gain of an ideal operational amplifier is infinite which means if there is a small change between the voltage on the input terminals it will drive the output to one of the supply rails. Following are the important properties of an ideal operational amplifier<sup>13</sup>

- Infinite open loop gain
- Infinite input impedance which will imply that the input terminals will not draw any current.
- Zero output impedance which implies that the operational amplifier can supply infinite amount of current i.e. it acts as a current buffer.

This is the ideal case. In general real operational amplifiers have an open loop gain ranging from  $10^4$  to  $10^8$ , with an input impedance is in range  $10^6$  to  $10^{13}\Omega$  and an output current limited to 100mA – 1A. The above properties of operational amplifiers are used extensively to build the potentiostat.

### **Operational amplifier feedback configurations:**

In a feedback configuration, the output is connected to the inverting input. This configuration determines the circuit operation and insures that the amplifier is stabilized. Further, in this configuration, the output of the operational amplifier will change to keep both the



input terminals at the same voltage. In the following list, a few of the feedback configuration used to build the potentiostat are discussed.

### 1. Inverting amplifier

Figure 20(a) shows the inverting amplifier configuration, where a feedback resistor  $R_f$  is connected between the inverting input and the output. Output voltage  $V_{out}$  is proportional to input current  $i_{in}$ . The non-inverting terminal is grounded hence the operational amplifier pulls the inverting terminal also to ground this is known as virtual ground. . In this configuration the feedback current is given by:

$$i_f = -i_{in} \text{ from Kirchoff's current law} \quad (5)$$

$$i_f = \frac{V_{out}}{R_f} \text{ and } i_{in} = \frac{V_{in}}{R_{in}} \quad (6)$$

$$\text{From the above two equations we have } V_{out} = -V_{in} \left[ \frac{R_f}{R_i} \right] \quad (7)$$

The above is the transfer function for an inverting amplifier configuration.

Figure 20(b) is also an inverting amplifier configuration but it also sums the three inputs, the feedback circuit is same as above but the current law at the summing point N is as follows

$$i_f = -[i_1 + i_2 + i_3] \quad (8)$$

$$V_{out} = - \left[ V_{in1} \left( \frac{R_f}{R_1} \right) + V_{in2} \left( \frac{R_f}{R_2} \right) + V_{in3} \left( \frac{R_f}{R_3} \right) \right] \quad (9)$$

If all resistor values are equal then we have

$$V_{out} = -[V_{in1} + V_{in2} + V_{in3}] \quad (10)$$

This configuration is known as summing amplifier.

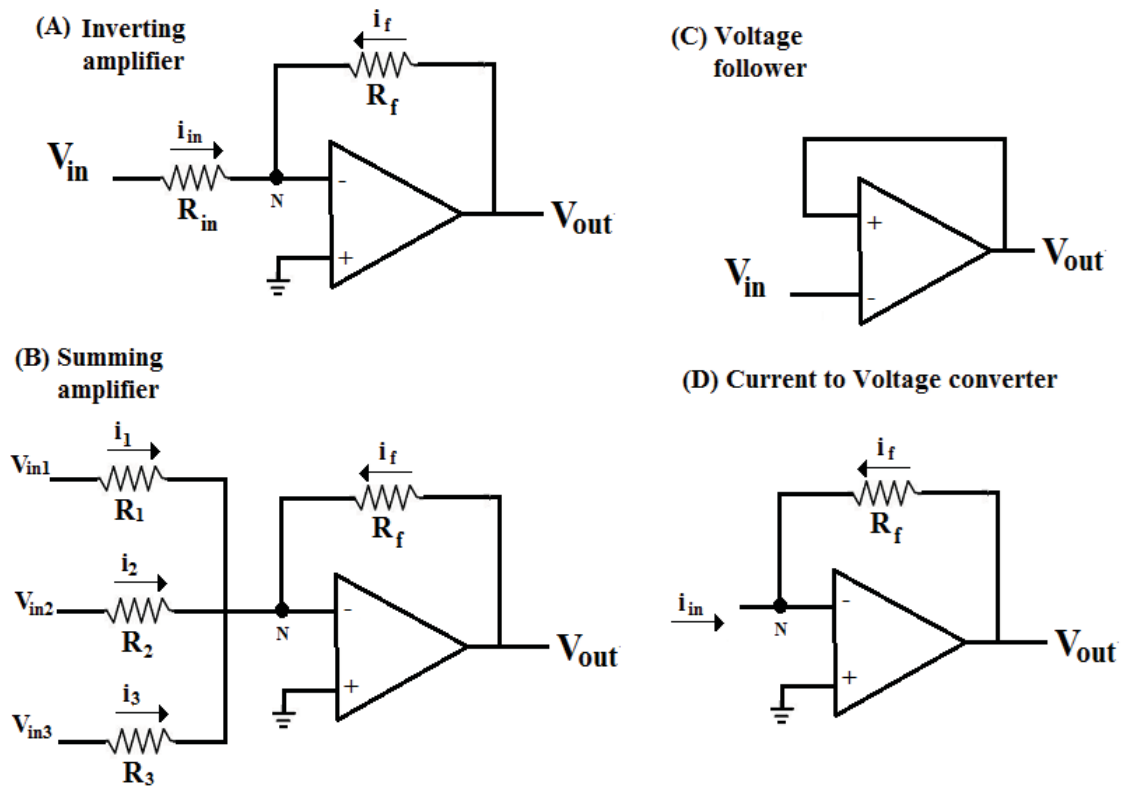


**Figure 20 Different feedback configurations of operational amplifiers**

2. Voltage follower:

Figure 20(c) shows the voltage follower configuration, in which the output is directly connected to the inverting terminal. The operational amplifier tries to keep both the inputs at the same voltage; due to the feedback output will now be equal to  $V_{in}$ . Hence in this configuration output just tracks the input and because of the high input impedance of the operational amplifier it draws no current.

3. Current to Voltage converter:

Figure 20(d) shows the current to voltage converter configuration. In this configuration the current input is connected to the inverting terminal, but the input terminals having

high impedance do not allow any current to flow through it hence all the current has to flow through the feedback resistor  $R_f$ .

$$i_f = -i_{in} \quad (11)$$

thus the output voltage will be proportional to the input current and is given as

$$V_{out} = -I_{in} \times R_f \quad (12)$$

Also this circuit makes the inverting input a virtual ground as the non-inverting terminal is connected to ground.

These configurations are used while building the potentiostat circuit for the three electrode sensor. The construction of the potentiostat and how it integrates with the sensor is discussed in detail in the sub-section 3.5.3.

### 3.6.2 Equivalent circuit of the sensor

Before going into the constructional details let us look at the equivalent circuit of the sensor. Figure 21 shows the equivalent circuit of the electrochemical cell. The actual equivalent circuit<sup>17</sup> is more complex than the one shown below but this is sufficient for small signal operation like ours.

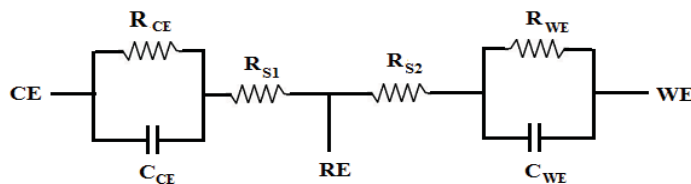


**Figure 21 Equivalent circuit of the electrochemical sensor**

$R_{CE}$  and  $R_{WE}$  are the charge transfer resistances,  $C_{CE}$  and  $C_{WE}$  are the double layered capacitance of the counter and working electrodes respectively<sup>18</sup>. The reference electrode is a non-polarizable electrode, it has no faradic reaction associated with it.  $R_{S1}$  and  $R_{S2}$  are the solution resistances

respectively. After an RC time constant the double layered capacitance will be charged up and the above circuit will reduce to two resistances one between CE and RE and the other between RE and WE. And we will be considering only these two resistances for circuit analysis of the potentiostat.

### 3.6.3 Construction of the potentiostat

The potentiostat should perform all the three tasks described at the beginning of this section. In order to achieve these goals the potentiostat has two major building blocks

1. Control amplifier: Responsible to control the potential difference between WE and RE
2. I/V Converter: responsible to measure the current from the WE and also maintains WE at virtual ground.

Figure 22 shows the circuit of a potentiostat with the control amplifier and the I/V converter sections shown clearly.

#### Control amplifier:

As stated previously the objective of control amplifier is to ensure that the cell potential  $V_{cell}$  tracks the applied potential  $V_{in}$ . The operational amplifiers OP1 and OP2 are a part of the control amplifier section. OP2 is configured as a voltage follower; it just tracks the cell potential and allows no current to flow through the RE.

$$V_{cell} = -V_{RE} \quad (13)$$

OP1 which is the main control amplifier is configured as an inverting summing amplifier with two summing inputs at node S, one is the input voltage ( $V_{in}$ ) from the Digital to Analog converter and the other is output of OP2, the sampled cell potential. The negative feedback

around OP1 is completed via the solution resistance between CE and RE. Voltage seen at node S is given as

$$V_s = \frac{V_{RE} + V_{in}}{2} \quad (14)$$

A property of the operational amplifier is that the output will change to keep both the inputs at the same voltage. The non-inverting terminal of OP1 is tied to ground hence if  $V_x$  is not zero

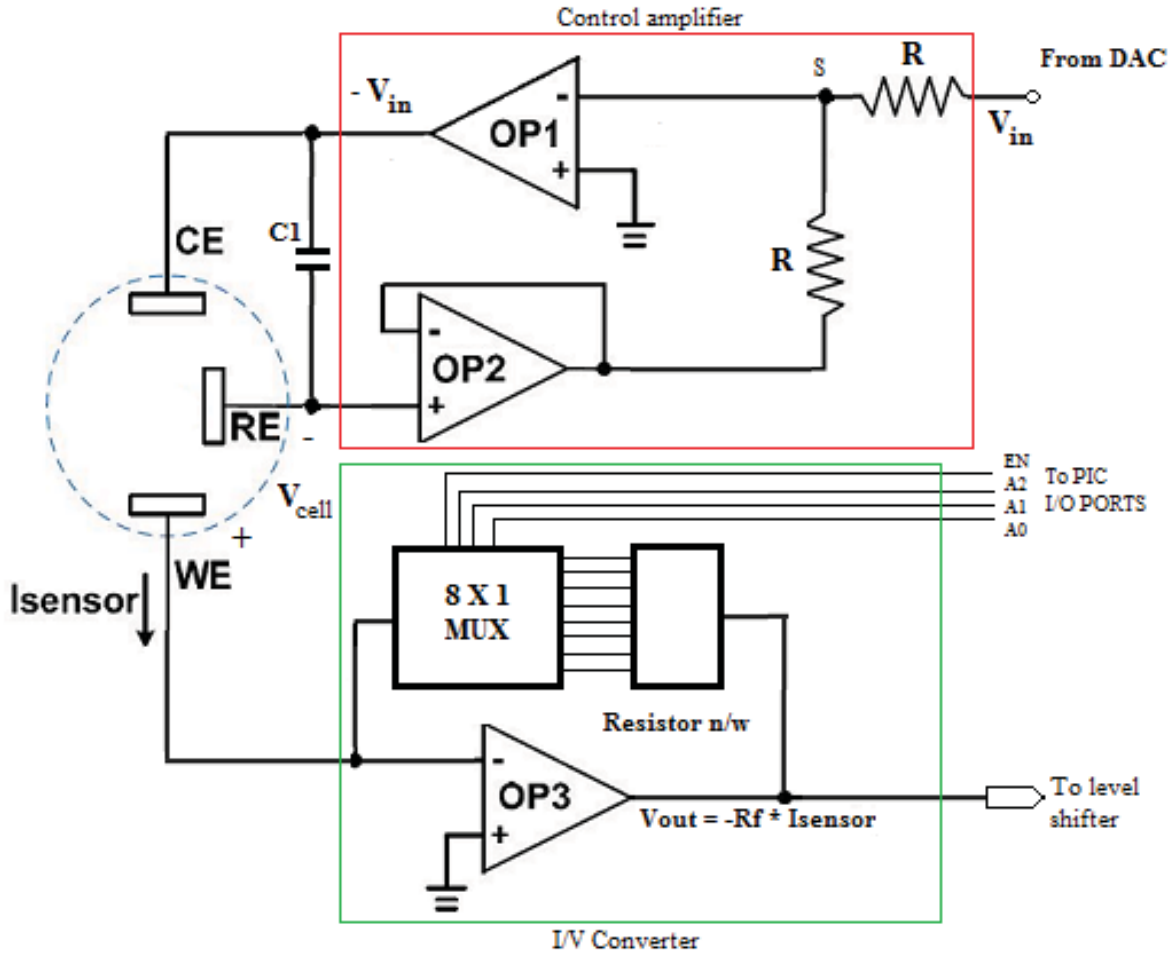


**Figure 22 Circuit diagram of potentiostat**

OP1 output will change in a manner to bring  $V_s$  back to zero i.e., virtual ground. From equations (13) and (14) it is obvious that  $V_s$  will be zero only when  $V_{cell}$  is equal to  $V_{in}$ . Hence OP1 current

output will change accordingly to make the cell potential equal to the applied potential. For example, consider that a potential of +1V is applied from the DAC OP1 delivers the required current to keep the cell at +1V, but if at some point due to the electrochemical reactions in the cell, the cell potential  $V_{cell}$  is higher than the +1V, OP1 decreases the current injected into the cell and eventually the cell potential will drop back to +1V. If the  $V_{cell}$  is less than the applied potential +1V then OP1 will inject more current until the cell potential becomes +1V. In this manner OP1 and OP2 ensures that the cell potential always tracks the applied potential  $V_{in}$ . A capacitor  $C_1$  is connected between AE and RE to remove any possible oscillation that might occur during the voltammetry process.

#### **I/V converter:**

As seen in Figure 22 OP3 is configured as a I/V converter. The non-inverting terminal of OP3 is wired to ground. Hence, OP3 ensures that WE is always at virtual ground. At the same time, the current from WE  $I_{sensor}$  is converted to a corresponding voltage as per the following equation

$$V_{out} = -I_{sensor} \times R_f \quad (15)$$

Where  $R_f$  is the value of the feedback resistor connected between the output and the inverting terminal of OP3. Since the range of current depends on the concentration of Zn in the sample solution, instead of using a single feedback resistor a network of resistors ranging from (1K $\Omega$  to 4M $\Omega$ ) is used along with a 8X1 multiplexer, to select one of the 8 resistors in the feedback loop. The multiplexer's select lines are controlled by the microcontroller and the software is programmed to automatically scale I to V converter by changing the select lines depending on the measurements made. The details circuit of the potentiostat using commercial operational amplifiers and multiplexers is described in the section 3.6.5.

### 3.6.4 Level shifter

The voltage value which corresponds to the current from WE need to be digitized and stored for quantification of Zn. This is done using the ADC module on the PIC18F8722 which was already discussed in section 3.3.5. The 10bit ADC on PIC18f8722 can measure only positive voltages between 0V to 5V. A level shifter has been incorporated using OP4, it up-shifts the output of I/V converter by 2.5V. The output of the level shifter is connected to the ADC for digitization. The software then converts the measured voltage back to its corresponding current value and stores it in the EEPROM. Figure 23 shows the level shifter configuration

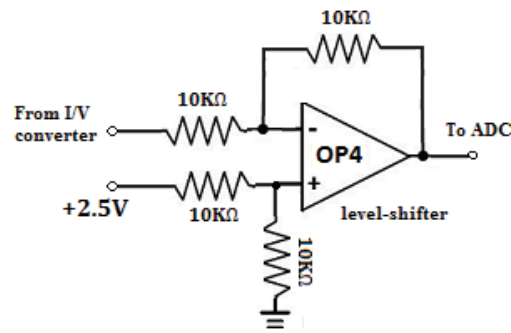


**Figure 23 +2.5V Level shifter**

### 3.6.5 OP484 operational amplifier and the potentiostat

The circuit for the potentiostat is developed using OP484 IC from Analog Devices® and ADG408 multiplexer IC also from Analog Devices®. OP484 is a quad, rail to rail operational amplifier. The four operational amplifiers on OP484 IC are used to construct the potentiostat circuit and the level shifter. Figure 24 shows the connections for OP484. To build the I/V converter an auto scaling feature has been implemented using an 8X1 MUX and a network of resistors as the feedback for the operational amplifier. Since the range of current that will be measured is unknown the software picks the correct resistor value following the Initialize\_MUX

pseudo code presented below. The ADC digitizes the measured current in terms of a voltage given by equation 15, if the measure voltage is in the range (0.3V – 2.2V) then the multiplexer has picked the right resistor value. Otherwise the feedback resistor value needs to be switched up or down. The procedure for doing so is described in the switch\_MUX pseudocode. A current measurement will be made at the end of each half cycle and the software checks at this point if the MUX lines have to be switched for the next measurement. The switch occurs if the measured

### Figure 24 Circuit diagram of OP484

### Initialize\_MUX:



**Switch\_MUX ( ADC\_voltage, select\_lines )**

Step1: **If** ((ADC\_voltage < 0.3V) && (select\_lines < 7))

    select\_lines ++;

**Else if** (ADC\_voltage > 2.2V && (select\_lines > 0))

    select\_lines--;

**Else**

**Exit;**

The conditions( select\_lines < 0 and select\_lines > 7) have been imposed to ensure that we do not enter a infinite loop if the current values are too high or too low.

Table 4 shows the feedback resistor values, corresponding current range and the select lines.

The circuit diagram for the resistor network and ADG408 multiplexer are shown in Figure 25.

**Table 4 Feedback resistor values and the corresponding current range**

Feedback resistor value	Current measured range		8X1 MUX select bits		
	Lower limit	Higher limit			
1K $\Omega$	400 $\mu$ A	1.5mA	0	0	0
3.3K $\Omega$	121 $\mu$ A	454 $\mu$ A	0	0	1
10K $\Omega$	40 $\mu$ A	150 $\mu$ A	0	1	0
30K $\Omega$	13 $\mu$ A	50 $\mu$ A	0	1	1
100K $\Omega$	4 $\mu$ A	15 $\mu$ A	1	0	0
330K $\Omega$	1.21 $\mu$ A	4.24 $\mu$ A	1	0	1
1.25M $\Omega$	320nA	1.2 $\mu$ A	1	1	0
4M $\Omega$	100nA	375nA	1	1	1

The select lined A0, A1 and A2 of the MUX are connected to RG0, RG1 and RG2 pins of the microcontroller respectively.

### 3.7 Memory module

Quantification of Zinc is done by measuring the peak current value in a voltammogram which is plotted as applied net current vs voltage. A current measurement is made in the stripping phase before each potential change and recorded as forward/reverse depending on when

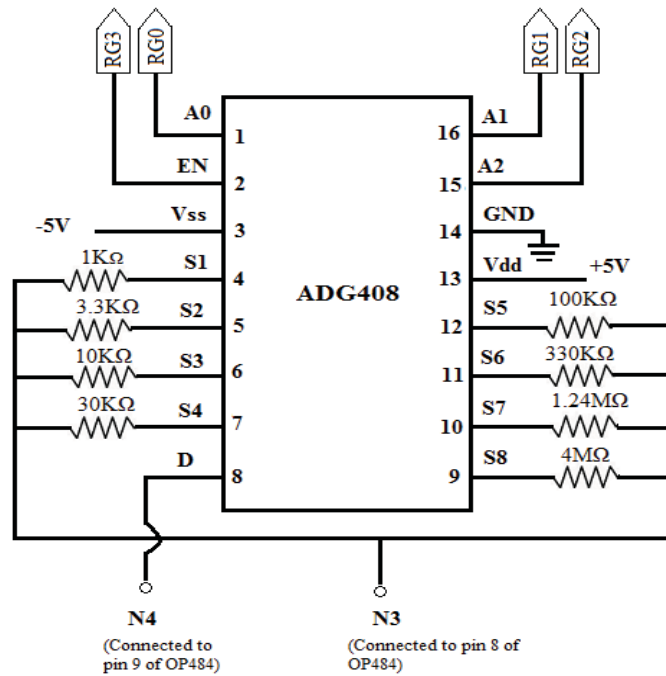


**Figure 25 Circuit diagram of ADG408 multiplexer**

the reading was made (positive/negative half cycle). And net current is computed as the difference between the forward and reverse current. These current values are digitized by the 10-bit ADC and the software converts that value into an ASCII format (which is readable on a computer). While these values are coming every half cycle they are buffered and stored into an EEPROM. Once the experiment is over all the values in the EEPROM are transferred onto an SD card. Then the data can be plotted on any data processor for analysis. The communication between the microcontroller and the memory module, which comprises of EEPROM and SD card, is established through the two SPI modules that have been discussed already.

### 3.7.1 25LC256 EEPROM

A 25LC256 serial EEPROM from Microchip® has been used, it has the following features<sup>19</sup>:

- 256Kbit memory which can be accessed by a serial SPI bus that has three signals Serial data in (SI), serial data out (SO) and a clock input (SCK).

- It has a 64bit page size.
- Access to the EEPROM is controlled by a chip select  $\overline{CS}$  input and communication to it can be paused by using the hold pin ( $\overline{HOLD}$ ).
- It has an internal write time of 5mS (maximum);
- It contains an 8-bit instruction register.
- It contains a write enable latch which must be set before any write operation. This is done by using WREN instruction.

Table 5 contains the instructions set for the EEPROM and Figure 26 shows the circuit connections between EEPROM and the microcontroller

**Table 5 Instruction set of 25LC256 EEPROM**

Instruction Name	Instruction Format	Description
READ	0000 0011	Read data from memory array beginning at selected address
WRITE	0000 0010	Write data to memory array beginning at selected address
WRDI	0000 0100	Reset the write enable latch (disable write operations)
WREN	0000 0110	Set the write enable latch (enable write operations)
RDSR	0000 0101	Read STATUS register
WRSR	0000 0001	Write STATUS register

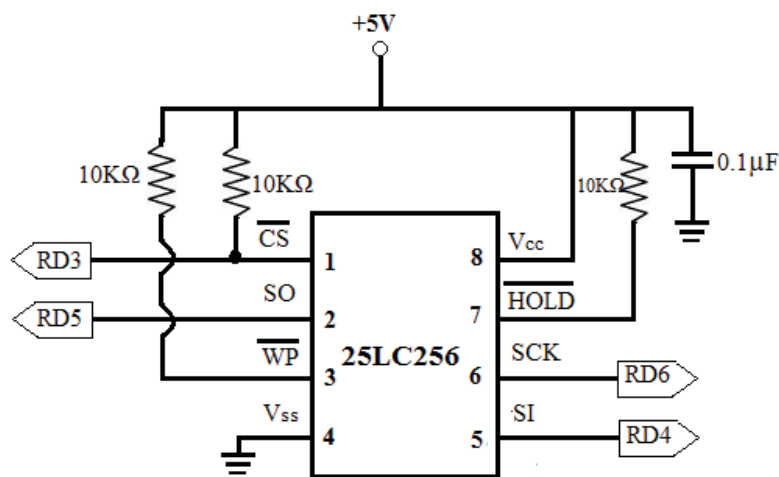
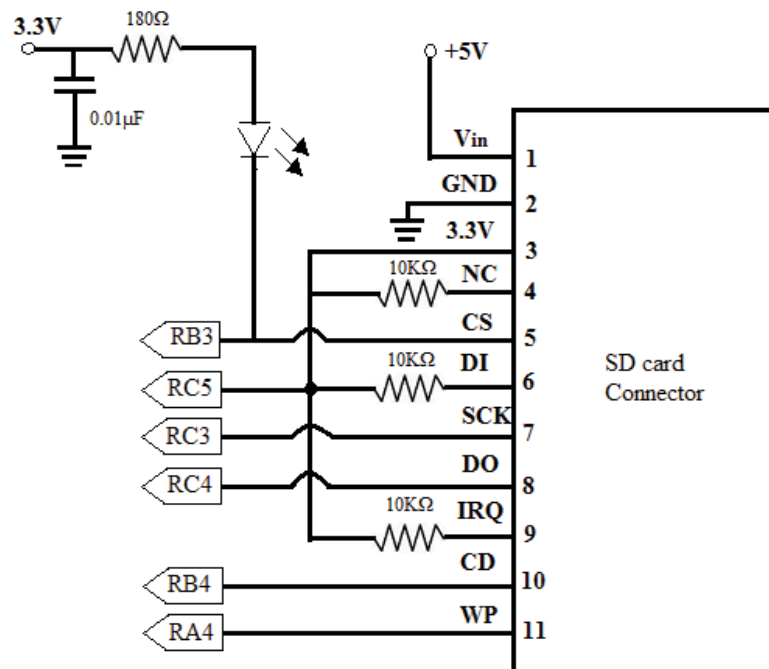


**Figure 26 Connections for 25LC256 EEPROM and the microcontroller**

### 3.7.2 SD card

The SD card also is interfaced to the microcontroller using SPI. In addition to the four signals (SI, SO, SCK and  $\overline{CS}$ ) it requires two additional signals card detect (CD) and write protect (WP). Hence the SD card requires six I/O pins of the microcontroller. The microchip's memory disk driver file system library<sup>20</sup> has been used for the communication between the SD card and the microcontroller. This is based on the ISO/IEC 9293 specifications which can support FAT16 and FAT32 file systems. SD cards sized below 2GB use FAT16 standard and FAT32 for



memories above 2GB. Figure 27 shows the circuit connections between the SD card holder and the microcontroller. The SD card holder also has a level translator and a 3.3V voltage regulator to facilitate the communication between the PIC18F8722 which is a 5V device and the SD card (which is a 3.3V device).

### 3.8 Power supply and Printed Circuit Board

All the peripheral devices require a positive (+5V) and a negative (-5V) power supply. The positive supply is derived from the PIC18 explorer development board. The negative (-5V) supply is constructed using a 9V alkaline battery, LM7905 voltage regulator and LM7660 voltage converter. Circuit diagram of the power supply is shown in Figure 28.

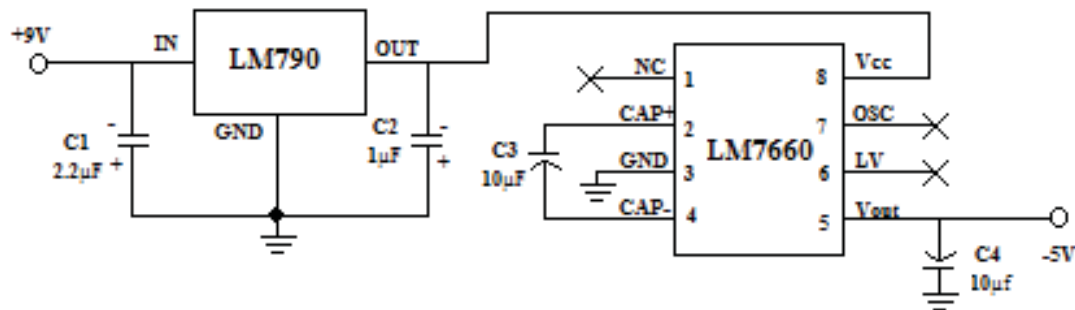
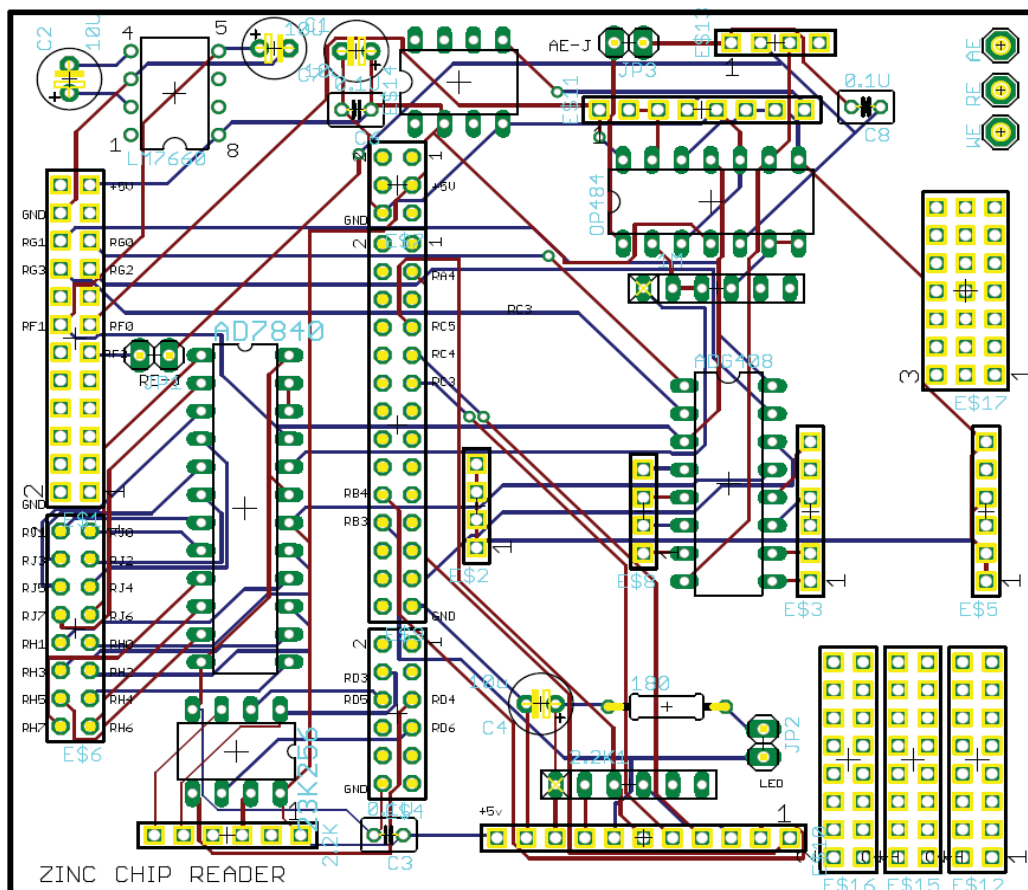


**Figure 28 negative (-5V) power supply circuit diagram**

A Printed circuit board has been designed to mount all the peripheral devices and the powers supply. Connections between PCB and PIC 18 explorer board is established via the PICtail connectors provided on the demonstration board. Layout of the PCB is shown in Figure 29.



## CHAPTER 4

### EXPERIMENTAL VERIFICATION

#### 4.1 Testing using sensor equivalent circuit

Prior to using the Point-Of-Care device with the three electrode sensor preliminary testing was done using the sensor equivalent circuit shown in Figure 21. The solution resistance has been varied over a range of  $1\text{K}\Omega$  to  $10\text{K}\Omega$  and the recorded V-I characteristics have been observed. The characteristic curve is expected to follow Ohm's law. Figure 30 shows an output plot when  $10\text{K}\Omega$  resistor was connected as the solution resistance, it can be noted that the slope of the curve is also  $10\text{K}\Omega$ . Thus the Point-Of-Care device has been validated using the equivalent circuit of the sensor.

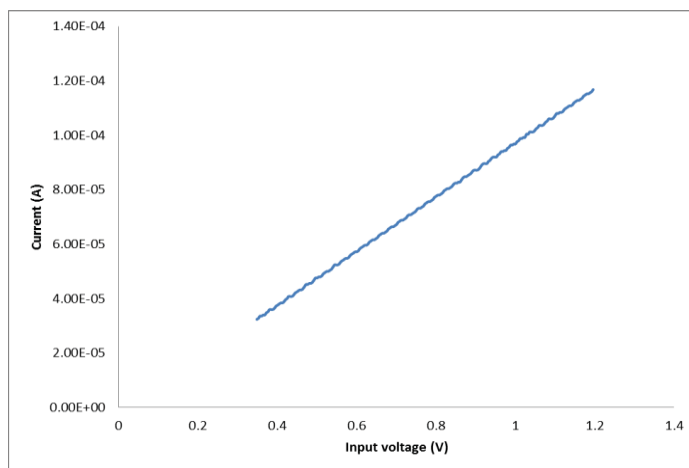


**Figure 30 V-I characteristics of the device using the sensor equivalent circuit**

#### 4.2 Experimental set-up

In order to validate the Point-Of-Care device to quantify Zinc, the device has been tested using Sodium Acetate buffer of pH 6 spiked with a given concentration of Zinc. The experimental set-up for conducting these experiments is shown in Figure 31, the Point-Of-Care device is

connected to the electrochemical sensor through a USB mini – B connector and alligator clips as shown.

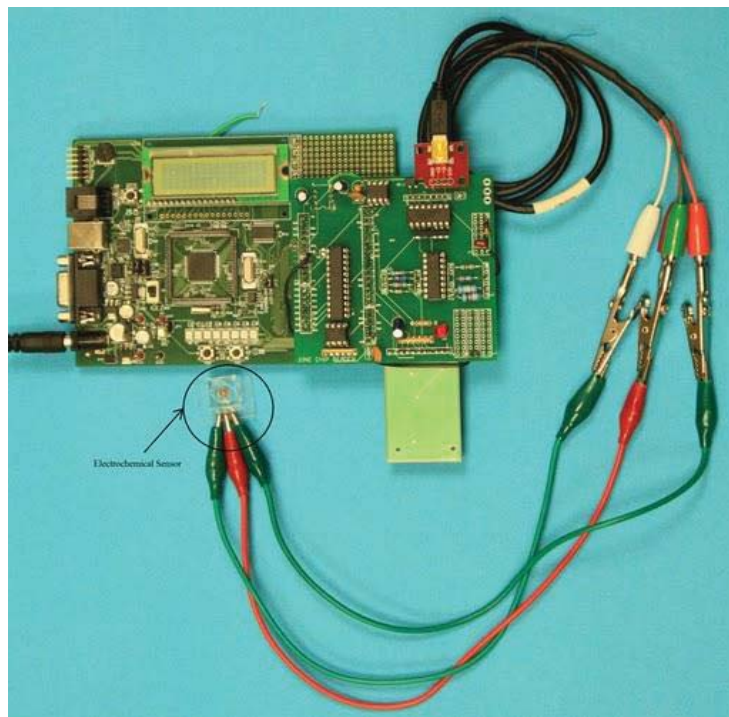


**Figure 31 Experimental set-up of the Point-Of-Care device**

Following experiments were performed to validate the device:

1. Sodium Acetate buffer of pH 6 spiked with three different Zn concentrations -  $10\mu\text{M}$ ,  $20\mu\text{M}$  and  $40\mu\text{M}$ .
2. For each concentration three reading are made and consistency of the measured peak current should be verified for reproducibility.
3. Sodium Acetate buffer of pH 6 will be spiked with Zinc and Cadmium, to prove that the Point-Of-Care device is able to distinguish other heavy metals in the solution.

And the results from the above experiments will be compared against the corresponding results from a bench-top potentiostat – Wavenow USB Potentiostat/Galvanostat from Pine Research Instruments.



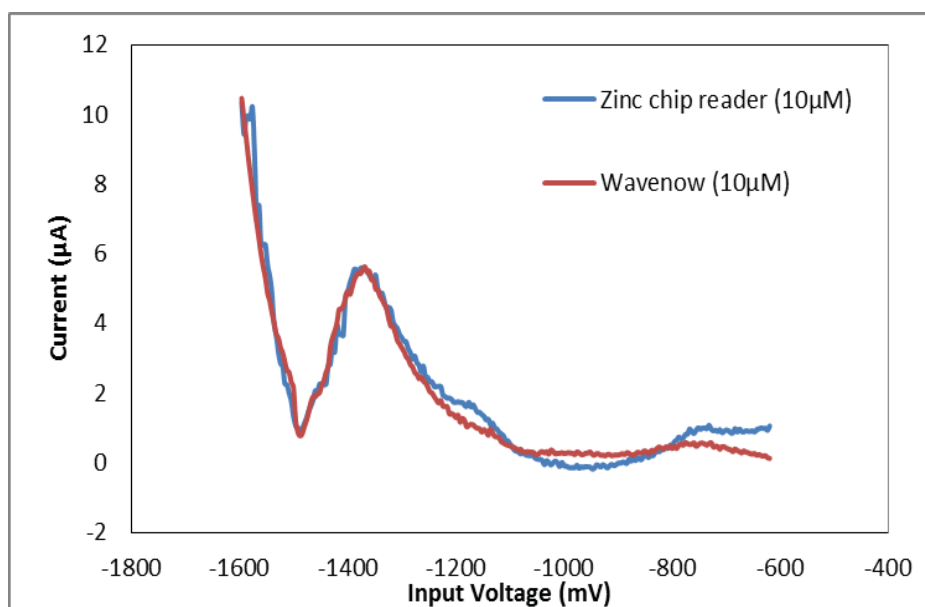
The input waveform parameters for all the below:

- Initial Voltage = -1600 mV
- Final Voltage = -600mV
- Step size = 4mV
- Pulse size = 25mV
- Frequency = 15Hz
- Preconcentration time = 600 s
- Quite time = 20 s

Before each measurement is made the sensor WE (Bi) must be plated, this is done by electroplating the WE using Bismuth plating solution by holding the potential at -800 mV for 240 s.

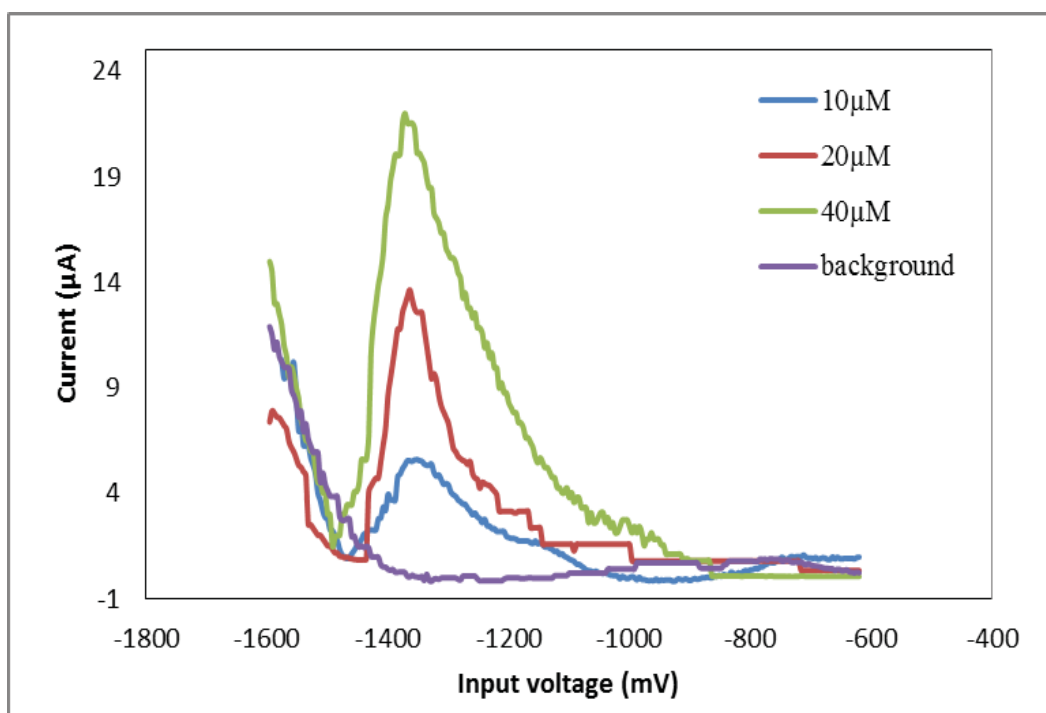
### 4.3 Results and discussion

Figure 32 shows the resulting voltammogram plotted as net current in  $\mu\text{A}$  vs. input voltage in mV concentration of  $10\mu\text{M}$  in an acetate buffer of pH 6. It can be inferred from Figure 32 that the Point-Of-Care device is able to track the voltammogram of the commercial Wavenow potentiostat very well.



**Figure 32 Voltammogram for  $10\mu\text{M}$  Zn in acetate buffer of pH 6 using Zinc chip reader and wavenow potentiostat**

Figure 33 shows the stripping peaks of Zn for three different concentrations (10 $\mu$ M, 20 $\mu$ M and 40 $\mu$ M) and it also shows the voltammogram for the acetate buffer of pH 6 without any Zn in it (marked as background).



**Figure 33 Voltammogram for SWASV of Zn concentrations from 10 $\mu$ M to 40 $\mu$ M spiked in an acetate buffer of pH6**

It can be observed that the Zn stripping peak occurs at about -1.368V and also that in plain acetate buffer there is no peak at that voltage, which is expected as there will not be any Zn in buffer. The peak current value must increase with increase in Zn concentration because the number of ions deposited on the electrode surface increases which eventually results in an increased current during stripping. It can be noted from Figure 33 that the peak current values increase with increase in concentration.

Three sets of experiments have been conducted for each concentration to account for the reproducibility of the results. Table 6 reports the peak current values of the three sets of experiments for different concentrations of Zn. It can be noted from the table that the

measurements have very less standard deviation and hence the device has very good reproducibility for a given concentration.

**Table 6 Peak current values for different concentrations of Zn**

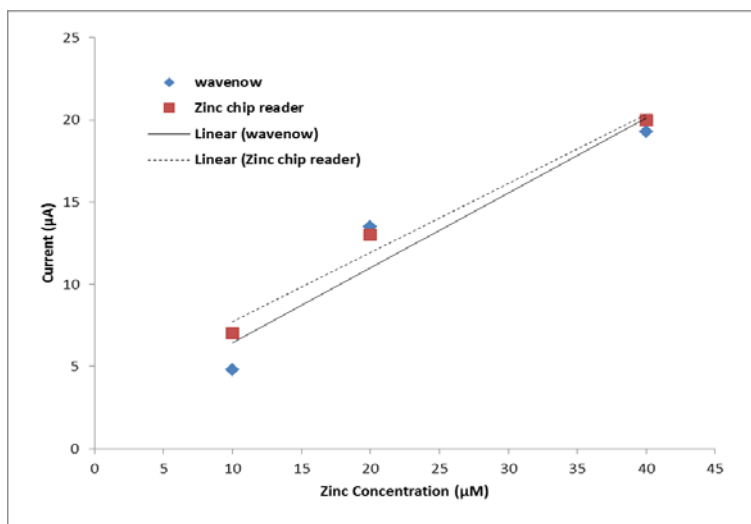
Concentration	Net current				Standard deviation
	Experiment 1	Experiment 2	Experiment 3	Average	
40 $\mu$ M	21.025	22.053	20.197	21.0917	0.4846
20 $\mu$ M	12.975	11.782	11.953	12.2367	0.5267
10 $\mu$ M	5.0975	4.697	5.213	5.0025	0.2211

Average peak current values from the above Table 6 are compared with the peak currents measured for the same concentrations using the wavenow potentiostat. These values are reported in Table 7, based on these values a calibration curve (measured peak current vs. concentration) is plotted for both the Point-Of-Care device and Wavenow potentiostat.

**Table 7 Peak current values for the three Zn concentrations of Point-Of-Care device and wavenow**

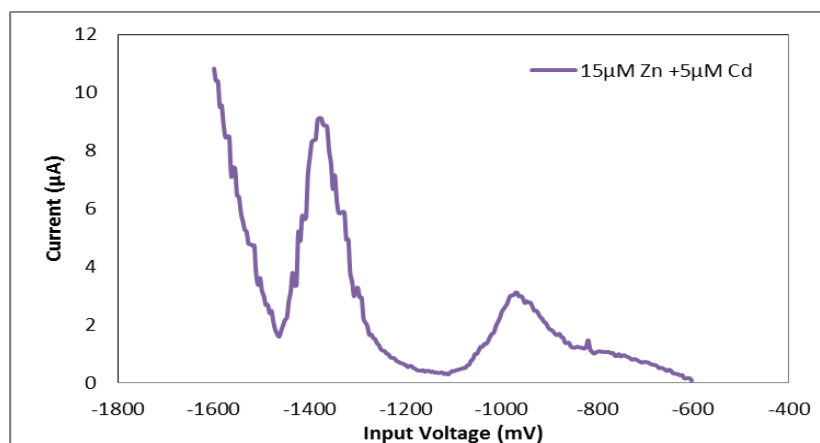
Concentration	Net current ( $\mu$ A)	
	Wavenow	Point-Of-Care device
40 $\mu$ M	19.2815	21.7103
20 $\mu$ M	13.4915	12.2367
10 $\mu$ M	4.797	5.0025

Figure 34 it shows that the calibration curves of these two devices. It can be observed that the calibration plots of the two devices are very similar with an error percentage of about 8.73%. This is percentage is acceptable since the device is able to quantify Zn and also is able to reproduce the results.



**Figure 34 Calibration curve's for the Point-Of-Care device and Wavenow**

In order to prove that the Point-Of-Care system is able to distinguish between Zn and other heavy metals that might be present in the sample solution, a Sodium acetate buffer of pH 6 is spiked with 15μM Zinc and 5μM Cadmium (Cd), has been tested. Figure 35 shows the voltammogram of the acetate buffer spiked with Zn and Cd. It can be observed that there are two stripping peaks one at -1.36V (corresponding to Zn) and the other at -0.95V (corresponding to Cd). Thus if the analyte has any other heavy metal present in it along with Zn the Point-Of-Care device is able to distinguish between them.



**Figure 35 Voltammogram for acetate buffer of pH 6 spiked with 15μM Zn and 5μM Cd**

## CHAPTER 5

### CONCLUSIONS AND FUTURE WORK

#### 5.1 Conclusion

A Point-Of-Care device for rapid quantification of Zn has been developed; it has a turnaround time of about 30 Minutes. It is very portable as it can work as a standalone device (does not require to be connected to a computer while the quantification process is in progress) and weighs only about 0.5lbs.

The calibration curve for our device is shown in Figure 36, the calibration plot has a sensitivity of  $0.545\mu\text{A}/\mu\text{M}$ . The Point-Of-Care device generated a linear increase in current for with increasing concentration of Zn in the analyte solution with a  $R^2 = 0.9873$ .

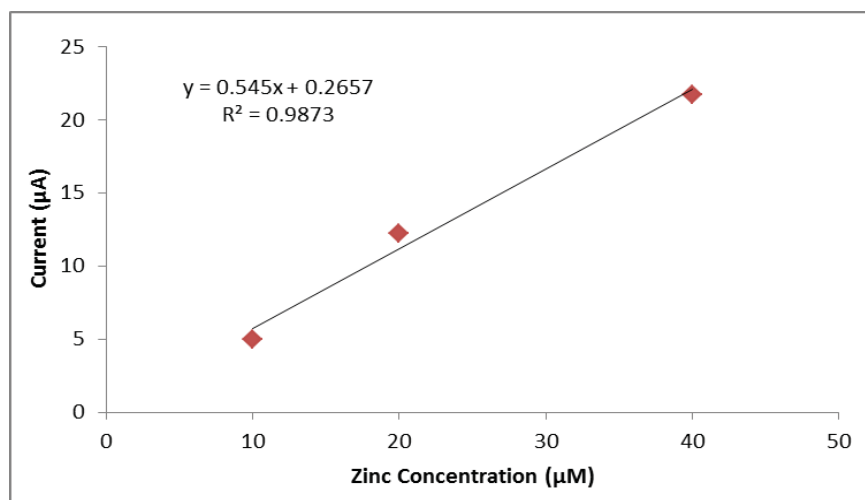


**Figure 36 Calibration curve of the Point-Of-Care device**

The Point-Of-Care device is able to accurately measure the concentration of Zn and is also able to distinguish between other heavy metals present in the analyte. The physiological range of Zn in blood serum is  $10\mu\text{M}$  to  $15\mu\text{M}$ <sup>Error! Bookmark not defined.</sup>, hence this device can be used to measure Zn in blood serum.

## 5.2 Future work

It can be noted from Figure 33 and Figure 35 that there is some digitization error in the measured current values and this error becomes prominent when the current approaches 0A, this is due to the 10 bit ADC which has a maximum offset error of  $\pm 3$  LSB. In order to achieve more accuracy in measurements a higher resolution bipolar ADC may be used instead, the use of bipolar ADC also eliminates some hardware such as level shifter in the potentiostat circuit.

In the current system the SWASV input parameters are changed in the source code, which is compiled and then programmed onto the microcontroller, instead a hardware interface may be developed to directly key in the input parameter values from the users.

Currently the quantification is done by loading the experimental values from SD card onto a computer and the plotting the voltammogram, a data processing algorithm can be developed and programmed onto the microcontroller that can analyze the output current vs. voltage data and directly display the concentration of Zn.

## References:

---

- <sup>1</sup> N. Z. Cvijanovich, J. C. King, H. R. Flori, G. Gildengorin and H. R. Wong, "Zinc homeostasis in pediatric critical illness," *Pediatric Critical Care Medicine*, vol. 10, pp. 29, 2009.
- <sup>2</sup> D. K. Heyland, N. Jones, N. Z. Cvijanovich and H. Wong, "Zinc supplementation in critically ill patients: a key pharmaconutrient?" *J. Parenter. Enteral Nutr.*, vol. 32, pp. 509, 2008.
- <sup>3</sup> R. S. Watson, J. A. Carcillo, W. T. Linde-Zwirble, G. Clermont, J. Lidicker and D. C. Angus, "The epidemiology of severe sepsis in children in the United States," *American Journal of Respiratory and Critical Care Medicine*, vol. 167, pp. 695, 2003.
- <sup>4</sup> H. R. Wong, N. Cvijanovich, G. L. Allen, R. Lin, N. Anas, K. Meyer, R. J. Freishtat, M. Monaco, K. Odoms and B. Sakthivel, "Genomic expression profiling across the pediatric systemic inflammatory response syndrome, sepsis, and septic shock spectrum," *Crit. Care Med.*, vol. 37, pp. 1558, 2009.
- <sup>5</sup> K. H. Ibs and L. Rink, "Zinc-altered immune function," *J. Nutr.*, vol. 133, pp. 1452S, 2003.
- <sup>6</sup> D. L. Knoell, M. W. Julian, S. Bao, B. Besecker, J. E. Macre, G. D. Leikauf, R. A. DiSilvestro and E. D. Crouser, "Zinc deficiency increases organ damage and mortality in a murine model of polymicrobial sepsis," *Crit. Care Med.*, vol. 37, pp. 1380, 2009.
- <sup>7</sup> P. Jothumuthu, R.A.Wilson, S.Sukhavasi, et. Al, "Point-Of-Care measurement of Zinc in blood serum", Conference on Miniaturized Systems for Chemistry and Life Sciences, pp. 1517 -1519, 2010.

---

<sup>8</sup> Y. Israel, T. Ofir and J. Rezek, "Determination of trace impurities in high-purity reagents by mercury thin-film anodic-stripping voltammetry," *Microchimica Acta*, vol. 69, pp. 151-163, 1978.

<sup>9</sup> W. Martinotti, G. Queirazza, A. Guarinoni and G. Mori, "In-flow speciation of copper, zinc, lead and cadmium in fresh waters by square wave anodic stripping voltammetry Part II. Optimization of measurement step," *Anal. Chim. Acta*, vol. 305, pp. 183-191, 1995.

<sup>10</sup> A.T. Maghasi, H.B. Halsall, W.R. Heineman and H.L. Rodriguez Rilo, "Detection of secretions from pancreatic islets using chemically modified electrodes," *Anal. Chim. Acta*, vol. 501, pp. 85 – 90, 2004.

<sup>11</sup> F. Vydra, K. Štulík and E. Juláková, *Electrochemical Stripping Analysis*. New York: John Wiley & Sons Inc., 1976.

<sup>12</sup> F. A. Settle, *Handbook of Instrumental Techniques for Analytical Chemistry*. Prentice Hall PTR, 1997.

"Handbook of instrumental techniques for analytical chemistry", F.A. Settle, ed., Prentice Hall PTR, v. 120 issue 26, 1998, p. 719 – 720.

<sup>13</sup> A. J. Bard and L. R. Faulkner, *Electrochemical Methods: Fundamentals and Applications*. New York: Wiley, 2001.

<sup>14</sup> PICDEM™ PIC 18 explorer demonstration board user's guide, Microchip, DS51721B, 2008.

<sup>15</sup> PIC18F8722 family datasheet, Microchip®, DS39646, 2008.



---

<sup>16</sup> LC<sup>2</sup>MOS complete 14-bit DAC AD7840, Analog devices, AD7850, 1989.

<sup>17</sup>S. M. Martin, F. H. Gebara, B. J. Larivee and R. B. Brown, "A CMOS-integrated microinstrument for trace detection of heavy metals," Solid-State Circuits, IEEE Journal of, vol. 40, pp. 2777-2786, 2005.

<sup>18</sup>M. M. Ahmadi and G. A. Jullien, "Current-mirror-based potentiostats for three-electrode amperometric electrochemical sensors," Circuits and Systems I: Regular Papers, IEEE Transactions on, vol. 56, pp. 1339-1348, 2009.

<sup>19</sup> 25AA256/25LC256 256K SPI Bus Serial EEPROM,DS21822F, Microchip, 2007.

<sup>20</sup> AN1045: Implementing file I/O function using Microchip's memory disk drive file system library, DS1045B, Microchip, 2008.